Accepted Manuscript

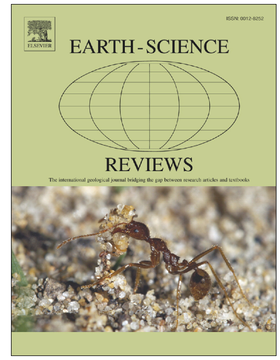

Jiangnan Orogen, South China: A ~970–820 Ma Rodinia margin accretionary belt

Jinlong Yao, Peter A. Cawood, Liangshu Shu, Guochun Zhao

PII: S0012-8252(18)30692-5
DOI: https://doi.org/10.1016/j.earscirev.2019.05.016
Reference: EARTH 2872

To appear in: *Earth-Science Reviews*

Received date: 11 December 2018
Revised date: 11 May 2019
Accepted date: 30 May 2019

Please cite this article as: J. Yao, P.A. Cawood, L. Shu, et al., Jiangnan Orogen, South China: A ~970–820 Ma Rodinia margin accretionary belt, Earth-Science Reviews, https://doi.org/10.1016/j.earscirev.2019.05.016

Jiangnan Orogen, South China: a ~970–820 Ma Rodinia margin accretionary belt

Jinlong Yao[a,b,c], Peter. A. Cawood[d,e], Liangshu Shu[c,*] lsshu@nju.edu.cn, Guochun Zhao[b,a]

[a]State Key Laboratory of Continental Dynamics, Department of Geology, Northwest University, Northern Taibai Street 229, Xi'an 710069, China

[b]Department of Earth Sciences, The University of Hong Kong, Pokfulam Road, Hong Kong SAR

[c]State Key Laboratory for Mineral Deposits Research, School of Earth and Engineering Sciences, Nanjing University, Nanjing 210093, China

[d]School of Earth, Atmosphere & Environment, Monash University, Melbourne, VIC 3800, Australia

[e]Department of Earth Sciences, University of St. Andrews, St. Andrews, KY16 9AL, UK

[*]Corresponding author.

Abstract

The Neoproterozoic Jiangnan Orogen in South China records a succession of arc-trench-basin assemblages culminating in accretion of the bounding Yangtze and Cathaysia blocks to form the stabilized South China Craton. The orogen can be traced over some 1500 km and extends up to 100 km across strike. It is divisible into three domains: the northeast domain (also referred to as the Huaiyu or Shuangxiwu Terrane), the central domain (Jiuling Terrane), and an undifferentiated southwest domain. The northeast domain contains arc type volcanic suites and I-type granitoids dated at ca. 970–850 Ma. It is interpreted as an intra–oceanic terrane based on the juvenile radiogenic isotopic signature of the igneous rocks, the absence of older detritus and inherited xenocrysts, and the presence of ophiolites along its southwestern and western margins. The central and southwest domains contain trench-arc-basin assemblages of clastic sedimentary units, mappable magmatic arc suites and ophiolitic mélanges (Sibao and equivalent groups) that range in age from ca. 880 to 820–815 Ma. The presence of old zircon grains within these two domains, both as detritus within sedimentary units and as inherited zircon in arc basalt, suggest they formed at convergent continental margins. S-type granites dated at 845–815 Ma are a distinctive element of the central and southwest domains. The ages of these granites overlap with convergent plate magmatism in the two domains, arguing against previous models for plume-rift and post-collisional geodynamic settings. Instead, these bodies likely formed in an accretionary orogenic margin setting in which granitic magmatism occurred in an extensional regime triggered by slab rollback. The slab-rollback process triggered mantle-sourced thermal input and partial melting of the older and buried arc-bounding basin sediments. Early Paleozoic S-type granites in the Lachlan and New England belts in eastern Australia and Jurassic ones in the Cordillera belt of the western US provide analogous geodynamic environments. Isotopic data indicate that the central Jiangnan domain experienced significant crustal growth, whereas in the southwest domain there was a greater degree of crustal reworking. The character and distribution of the early

Neoproterozoic sedimentary and igneous succession in the orogen suggests it represents a ca. 970–820 Ma accretionary orogen. Upper age limits on the Jiangnan Orogen are provided by a regional angular unconformity in the central and southwest domains at ca. 810–805 Ma, and in the northeast domain at ca. 825 Ma, along with the overlying bimodal volcanic and clastic sedimentary successions mostly dated at ca. 810–730 Ma. Thus, timing of final assembly of South China displays variations across the Jiangnan Orogen, from ca. 825 Ma in the northeast to ca. 820–805 Ma in the central and southwest of the orogen. Post-assembly successions are parts of the Nanhua Basin and are interpreted to have formed during regional lithospheric extension across the eastern and central South China Craton.

The age patterns across the South China Craton are indicative of northwest directed accretion of fragments and suggest an external rather than an internal position of the craton within the assembled Rodinia supercontinent. Paleomagnetic data, regional correlations and sedimentary records are consistent with a position along the northern margin of Rodinia, adjacent to India and Australia. The Jiangnan Orogen recorded the accretion of trench-arc assemblages and ultimately the Yangtze Block to the Cathaysia Block that was already located on the margin of Rodinia. The Panxi-Hanan belt, which lies along the western and northwestern margin of the Yangtze Block, formed on the upper plate to a subduction system that both overlaps with, and is younger than, the Jiangnan Orogen. The belt provides a record of ongoing accretion on the Rodinia margin until the mid-Neoproterozoic.

Keywords: Neoproterozoic Jiangnan Orogen; South China; Rodinia; accretionary orogeny; juvenile arc; convergent continental margin; S-type granites

1. Introduction

Orogenic belts are divisible into collisional (Alpine-Himalayan) and accretionary (non-collisional or Andean) types and provide the long-term geological archive of crustal growth and continental assembly (Windley, 1992; Collins, 2002; Cawood et al., 2009, 2016). Typical examples for the accretionary type include the Phanerozoic Terra Australis Orogen, the Central Asian Orogen, and the Cordilleran Orogen (Xiao et al., 2003, 2015; Cawood, 2005, 2011; Collins and Richards, 2008;). Determination of orogenic types, largely based on patterns of sedimentation, igneous activity, ophiolites, metamorphism and deformation, are crucial in understanding the drivers involved in continental generation and preservation (e.g. Cawood et al. 2013a).

The South China Craton has been variously linked with the Precambrian supercontinents of Columbia/Nuna, Rodinia and Gondwana (Zhao et al., 2002, 2018a; Li et al., 2008b; Cawood et al., 2013, 2018; Merdith et al., 2017). It is divisible into three Precambrian tectonic units, the Yangtze and Cathaysia blocks and the intervening Neoproterozoic Jiangnan Orogen (also referred to as the Jinning or Sibao Orogen) (Guo et al., 1989; Shu and Charvet, 1996; Zhao and Cawood, 1999, 2012; Wang et al., 2006, 2012a, 2014b; Li et al., 2008a, 2009; Cawood et al., 2013, 2018; Yao et al., 2014a, 2016a; Zhao, 2015) (Fig. 1). The Jiangnan Orogen includes a number of convergent plate margin successions that ultimately resulted in assembly of the Cathaysia and Yangtze blocks (e.g. Guo et al., 1996; Li et al., 2009; Zhao et al., 2011; Shu, 2012; Charvet, 2013; Wang et al., 2014b; Yao et al., 2015; Zhang and Wang, 2016). Shortly after assembly, the Jiangnan Orogen and Cathaysia Block underwent regional extension, resulting in development of the Nanhua rift basin (Wang and Li, 2003; Li et al., 2005; Shu, 2012; Wang et al., 2012c; Zhao and Cawood, 2012 and references therein; Yao et al., 2014b; Qi et al., 2019). The overall tectonic evolution of the Jiangnan Orogen, including timing and nature of arc-trench successions and related subduction polarity, age of final assembly, geodynamics of S-type granites, and the role of the orogen within the supercontinent cycles, are disputed (Li et al., 1999, 2003a, 2003b, 2008b; Shu et al., 2006, 2019; Greentree et al., 2006; Wang et al., 2006, 2013e, 2019; Wu et al., 2006; Zheng et al., 2007, 2008a; Zhao et al., 2011; Zhang et al., 2012b, 2013b; Yao et al., 2013, 2014a, 2016b; Zhao, 2015; Cawood et al., 2018). Two end-member tectonic models have been proposed for South China involving 'plume rifting' and 'subduction-collision' settings and reflect uncertainty in age and affinities of the rock units within South China. The former model argues for assembly of South China by ca. 880 Ma associated with Rodinia assembly (Li et al., 2002, 2007, 2009), followed by the initiation of extension related to breakup of the supercontinent at around 860 Ma (Li et al., 2003b, 2008a, 2008b; Yang et al., 2015). The subduction-collision model suggests final collisional assembly of the Yangtze and Cathaysia continental blocks at ca. 830 Ma, resulting in deformation and metamorphism of older successions in the Jiangnan Orogen, and the generation of ca. 835-815 Ma S-type granites in the belt (e.g. Wang et al., 2006, 2014c, 2018; Zhao et al., 2013). A few researchers have suggested magmatic arc activity in the Jiangnan Orogen continued to ca. 750 Ma, with final continental assembly not occurring until after this time (e.g. Lin et al., 2016). However, available data and observations, especially those published in recent years, including convergent plate margin successions with an upper age limit at least as young as ca. 820 Ma (e.g. Zhou et al., 2009; Wang et al., 2014b, 2015a, 2016b; Zhang et al., 2012c, 2015), and a regional unconformity at ca. 815–805 Ma in the southwest and central Jiangnan domains and at ca. 825 Ma in the northeast Jiangnan domain (Gao et al., 2008, 2011, 2014; Yao et al., 2013, 2015), along with ophiolitic mélange and arc magmatism as young as ca. 830–825 Ma (Zhang et al., 2012b, 2012c; Chen et al., 2014; Wang et al., 2014a, 2015a), partially disagree with age relationships outlined in all three models.

The aim of this paper is to document the tectonostratigraphic evolution of the Jiangnan Orogen, including litho-stratigraphic sequences, magmatic suites, metamorphic and structural events, and the geochemical and isotopic character of units. We concentrate on relations and data patterns across the orogen and South China. From these results, we address the inconsistency of previous models and provide constraints on the overall geodynamic evolution of the orogen, along with position of the South China Craton with respect to the Rodinia supercontinent.

2. Geological setting

The South China Craton is composed of the Yangtze Block to the northwest and the Cathaysia Block to the southeast, separated by the Jiangnan Orogen (Guo et al., 1989; Shu and Charvet, 1996; Wang et al., 2013e; Zhang et al., 2013b; Cawood et al., 2018). In this study, the boundary of the Jiangnan Orogen and the Cathaysia Block is considered to be the Shaoxing-Jiangshan-Pingxiang-Longsheng fault zone, which is interpreted as a Neoproterozoic structure (Fig. 1; Shu et al., 2015; Yao et al., 2016a). In detail, the position of this boundary fault is disputed due to poor exposure of Precambrian lithologies (Wang et al., 2013f; Shu et al., 2014; Guo and Gao, 2016). The boundary between the Jiangnan Orogen and the Yangtze Block is also poorly defined, and is herein taken as the Shitai-Jiujiang fault zone based on the distribution of exposed early to middle Neoproterozoic successions (Fig. 1).

The Yangtze Block includes minor exposures of metamorphosed Archean- early Paleoproterozoic TTG suites, and igneous and sedimentary successions that extend sporadically along the northern and western margins of the block, including the Kongling Complex, Yudongzi Group, Houhe complex and Huangtuling granulites (Fig. 2; Gao and Zhang, 1990; Qiu et al., 2000; Zheng et al., 2006; Wu et al., 2009; Sun et al., 2008; Zhao & Cawood, 2012 and references therein). These basement rocks are enveloped by Paleoproterozoic or younger successions within the Panxi-Hannan Belt along the northern and western southern margins of the block, as well as those of the Jiangnan Orogen in the southeast margin (Dong et al., 2011, 2012; Cawood et al., 2018; Zhao et al., 2018;). In the southwestern Yangtze Block, metamorphosed volcanic and sedimentary units formed at 1740–1503 Ma and are referred to the Dahongshan and Dongchuan groups (Fig. 2; Greentree and Li, 2008; Zhao et al., 2010), which are in fault contact with the ca. 1.23–1.0 Ga Kunyang and Huili groups (Sun et al., 2009; Zhao et al., 2010). Younger units in the Panxi–Hannan Belt are mostly composed of mafic to intermediate volcanic rocks, volcaniclastic sedimentary rocks and intrusives with subduction related chemical signatures, mostly within the age range of ca. 1.0–0.75 Ga (Zhou et al., 2002, 2006; Sun et al., 2009; Dong et al., 2012, 2017; Cai et al., 2014, 2015; Wang et al., 2016c; Zhao et al., 2018a, 2018b; Sun et al., 2019). All these successions are overlain by the upper Nanhua System (ca. 720 Ma to 630 Ma) and Sinian Group (ca. 630-542 Ma).

Archean rocks are not exposed in the Cathaysia Block but may be present at depth on the basis of Archean xenocrysts in mafic rocks and granites intruding the block (Yu et al., 2009; Zheng et al., 2011; Li et al., 2018), as well as detrital zircon grains of this age in the Neoproterozoic to Phanerozoic metasedimentary units (Zhao and Cawood et al., 1999; Yao et al., 2011). The oldest exposed lithologies in the block are minor 1.93–1.7 Ga igneous suites in east Cathaysia that are referred to as the Badu Complex and are enveloped by variably metamorphosed middle Neoproterozoic assemblages (Fig. 2; Zhao and Cawood, 1999; Shu et al., 2008; Yu et al., 2009; Yao et al., 2017). Earlier geological investigations suggested exposures of widespread Mesoproterozoic sequences in east Cathaysia, but new zircon U-Pb data established them as Neoproterozoic (Wan et al., 2007; Yang and Jiang, 2018). Mesoproterozoic sedimentary and intrusive rocks only occur on Hainan island (ca. 1.4–1.2 Ga; Li et al., 2008c; Wang et al., 2015b; Zhang et al., 2019), and were metamorphosed at ca. 1.3–1.0 Ga (Yao et al., 2017). Early Neoproterozoic rock suites, including meta–rhyolite, amphibolite and meta–basaltic rocks, sporadically occur in the Yunkai and Wuyi domains of the Cathaysia Block and display consistent subduction affinity, with their ages concentrated at ca. 1.0–0.9 Ga along with minor activity at ca. 840 Ma (Shu et al., 2008; Wang et al., 2013e and references therein; Xia et al., 2017 and references therein; Wang et al., 2018). Peraluminous gneissic granites dated at ca. 980–910 Ma have also been reported from localities within the block (Wang et al., 2014 and refences therein). Investigations on Middle Neoproterozoic magmatic suits (0.82–0.72 Ga) are limited to east Cathaysia, which display extension related geochemical signatures (Li et al., 2005; Shu et al., 2011; Xia et al., 2017 and references therein; Qi et al., 2019). Nanhua systems are also well preserved in the middle and western Cathaysia Block (referred to as the Shenshan and equivalent groups), and consist of schist, gneiss and minor quartzite, meta-sedimentary rocks and meta-basaltic rocks, along with marble and amphibolite, but with poorly constrained ages (Li et al. 2009; Shu et al., 2011; Zhang et al., 2013). These litho-stratigraphic sequences are unconformably covered by the Nanhua System and Sinian Group, along with early Paleozoic successions (Fig. 2; Shu et al., 2014; Qi et al., 2018).

The Jiangnan Orogen is here defined as a suite of deformed and metamorphosed early to earliest middle Neoproterozoic igneous and sedimentary suites, along with sheared I- and S-type granitic intrusions (Figs. 2, 3, 4; Guo et al., 1989; Shu et al., 1995, 2019; Shu and Charvet, 1996; Wang and Li, 2003; Charvet, 2013). Latest Mesoproterozoic volcanic rocks, referred to as the Tieshajie Group, have also been locally reported from areas within the Shaoxing - Jiangshan fault zone (Li et al. 2011, 2013). But the group are comparable to the protolith of the Zhoutan Group that constitutes the Cathaysia Block. Therefore, the tectonic affinity of the Tieshajie Group is unclear. Variations in ages of lithologies and relations across the Jiangnan Orogen, along with distribution of ophiolitic mélanges, suggest division into three domains: a northeast domain (Huaiyu Terrane), a central domain (Jiuling Terrane) and a southwestern domain (Fig. 1; Shu et al., 1995; Yao et al., 2013, 2016a). The boundary fault between the northeast and central domains is the early Neoproterozoic Northeast Jiangxi ophiolitic suture zone (Fig. 1; Shu, 2012; Yao et al., 2015), whereas that between the central and southwest domains is the inferred Miluo-Xiangtan fault (Fig. 1; Shu et al., 1995). The southwestern and northeastern extensions of the belt are covered by Phanerozoic strata (Fig. 1).

3. Lithostratigraphic sequences

Primary rock units exposed in the Jiangnan Orogen are from northeast to southwest referred to as the Shuangxiwu, Shuangqiaoshan, Shangxi, Lengjiaxi, Fanjingshan and Sibao groups, which record the evolution of the orogen (Figs. 2, 3, 4; BGMRJX, 1984; BGMRGX, 1985; BGMRGZ, 1987; BGMRHN, 1988; BGMRZJ, 1989; Zhou et al., 2014). Rock units within the orogen consist mainly of deformed clastic sedimentary rocks, volcanic rocks and their intrusive equivalents. In addition, minor ophiolitic mafic-ultramafic assemblages, limestone and deep-sea chert occur within the Shaoxing-Jiangshan and Northeast Jiangxi suture zones (Shu et al., 1994, 1995; Zhao et al., 2011; Zhao and Cawood, 2012 and references therein; Yao et al., 2015, 2016a). I- and S- type granitic intrusions also occur within the orogen (Li et al., 2003a; Wang et al., 2006; Ye et al., 2007; Yao et al., 2014a, 2016b). In detail, the lithostratigraphic character of the domains varies: the northeast domain (Huaiyu Terrane) is composed largely of deformed volcanic rocks, whereas the central and southwest domains are dominated by deformed clastic sedimentary rocks (Figs. 2, 3, 4). All the units have experienced regional greenschist facies metamorphism. The overall age range of lithologies within the orogen is from ca. 970 to 820 Ma, based on ages of volcanic horizons, igneous intrusions, and deposition of sedimentary successions constrained by maximum depositional ages of detrital zircons and subsequent overprinting relationships (Wang et al., 2003, 2007, 2010, 2013a, 2014a, 2014b, 2016b; Zheng et al., 2008b; Zhou et al., 2009, 2014; Li et al., 2009, 2016b, 2016c; Zhou et al., 2009, 2014; Gao et al., 2010, 2011; Zhang et al., 2012b, 2012c, 2018; Yao et al., 2013, 2015; Yin et al., 2013; Ma et al., 2016; Zhang and Wang, 2016; Xin et al., 2017; Su et al., 2018a, 2018b; Shu et al., 2019).

The Jiangnan Orogen is unconformably overlain by a succession of clastic sedimentary rocks along with some bimodal igneous rocks, which together constitute the Nanhua Basin (referred to as the lower Nanhua System in Chinese literature). In the Jiangnan region, these include from east to west the Heshangzhen, Dengshan, Likou, Banxi, Xiajiang and Danzhou groups (Figs. 2, 3, 4; BGMRJX, 1984; BGMRGX, 1985; BGMRHN, 1988; BGMRZJ, 1989; Shu et al., 1995; Wang and Li, 2003). This succession accumulated between ~825-805 Ma to 730 Ma (Wang et al., 2012b, 2013a, 2015, 2017; Gao et al., 2011; Shu, 2012; Xu et al., 2014b; Zhou et al., 2014; Yao et al., 2015; Yan et al., 2015; Ma et al., 2016; Su et al., 2018a), with the upper age limits ranging from ca. 760 Ma in the northeast to ca. 730 Ma in the southwest (Fig. 2). Bimodal igneous suites, containing two end members of basalt and rhyolite and their intrusive equivalents, yield ages in the range of ca. 800–760 Ma (Li et al., 2003b, 2008a; Wang et al., 2012c; Yao et al., 2014b; Zhang et al., 2018). These bimodal igneous suites occur within the Heshangzhen and equivalent groups in east Jiangnan and are thus assigned to the Nanhua rift basin succession. Elsewhere in the Jiangnan and Cathaysia regions, coeval rifting type diabase and basalt have been reported, but are not associated with felsic end members (Li et al., 2005; Wang et al., 2008; Shu et al., 2011). The units of the Nanhua Basin are essentially undeformed and unmetamorphosed (Fig. 4). The basin succession is overlain by platform strata of Sinian (corresponding to the Ediacaran) age, and extending from ca. 650–542 Ma (Fig. 2, 4). The units of the Nanhua Basin are distributed across the Cathaysia Block and Jiangnan Orogen, whereas those of Sinian age extend across South China (Fig. 2).

3.1 Northeast domain (‘Huaiyu’ or ‘Shuangxiwu’ Terrane), Jiangnan Orogen

The northeast domain of the Jiangnan Orogen contains the Shuangxiwu Group (Figs. 2, 3, 4), which is composed of a series of mafic to felsic volcanic rocks. Minor ophiolitic mafic-ultramafic suites and deep-sea chert occur along the Shaoxing-Jiangshan and Northeast Jiangxi fault zones that define the southeast and western margins of the domain, respectively (Fig. 3; Shu 1995; Li et al., 2009; Yao et al., 2016b). An undated thin layer of clastic rocks also occurs at the top of the group (BGMRZJ, 1989). LA-ICP-MS zircon U-Pb ages of 952 ± 5 Ma and 954 ± 8 Ma, 904 ± 8 Ma and 906 ± 10 Ma have been obtained from mafic-intermediate volcanic suites in the lower Shuangxiwu Group (Chen et al., 1991, 2016), as well as a whole rock Sm-Nd isochron age of 978 ± 44 Ma (Zhang et al., 1990). Andesitic rocks and hornblende schist from the middle to upper part of the Shuangxiwu Group yielded zircon ages of 926 ± 15 Ma and 891 ± 12 Ma (Li et al., 2009), 879 ± 10 Ma (Yao et al., 2014c), and 871 ± 7 Ma and 864 ± 14 Ma (zircon U-Pb, Yao et al. 2015). Tonalite-granodiorite plutons and quartz diorite dated at ca. 907 Ma and ca. 854 Ma are also present within the group (Ye et al., 2007; Yao et al., 2016b).

The Shuangxiwu Group has experienced extensive deformation and is unconformably overlain by the Heshangzhen Group (Pt3h) (Figs. 3, 4; BGMRZJ, 1989), the basal unit of the Nanhua Basin. Volcanic layers from the lower Heshangzhen Group are dated at 824 ± 5 Ma (SHRIMP zircon U-Pb, Zhang et al., 2015), whereas those in the middle and upper parts of the group are dated at ca. 802 Ma, ca. 790 Ma and ca. 767 Ma (Figs. 3, 4; Gao et al., 2008, Li et al., 2008a), consistent with detrital zircon ages obtained from clastic rocks within the group (Yao et al., 2013; Wang et al., 2013a).

3.2 Central domain (Jiuling Terrane), Jiangnan Orogen

The main litho-stratigraphic units in the central domain of the orogen are the Shangxi, Shuangqiaoshan and Lengjiaxi groups (BGMRJX, 1984; BGMRHN, 1988). These units comprise a similar succession of clastic meta-sandstone, meta-siltstone and slate, as well as various meta-tuffaceous layers that yield zircon U-Pb ages of 822 Ma ± 10 Ma (SHRIMP zircon U-Pb; Gao et al., 2011) and 825 ± 7 Ma (LA-ICP-MS zircon U-Pb; Yin et al., 2013). Minor mappable layers of basalt, diabase and high Mg andesite in the Shuangqiaoshan and Lengjiaxi groups from the southern margin of the domain yield ages in the range 870–825 Ma (Figs. 1, 3, 5; e.g., Shu et al., 1995; Zhang et al., 2012c, 2013c; Sun et al., 2017). A gabbro-diorite complex from the eastern margin of the domain is dated at ca. 870–860 Ma (Cui et al., 2017). Rocks of the domain are extensively folded and unconformably overlain by the undeformed Likou, Dengshan and Banxi groups of the Nanhua Basin (Figs. 2, 3, 4) (BGMRJX, 1984; Zhou et al., 2015; Yao et al., 2019). In the central Hunan area, a layer of volcanoclastic rocks, mainly composed of volcanic conglomerate, slate and meta–siltstone, occurs in the lowest Banxi Group and was deposited at some time after ca. 822 Ma (BGMRHN, 1988; Zhang et al., 2012c). Some studies refer to this layer as an independent unit, the Cangshuipu Group, which is related to final collisional assembly of South China (Pan et al., 1988; Zhang et al., 2012). These overlying successions have maximum depositional ages of ca. 810–800 Ma, based on the youngest detrital zircons (Wang et al., 2013b, 2015a, 2017; Yan et al., 2015; Sun et al., 2018) and tuffaceous layers (803 ± 8 SHRIMP Zircon U-Pb, Gao et al., 2011).

3.3 Southwest domain, Jiangnan Orogen

The southwest domain of the Jiangnan Orogen contains the Sibao and Fanjinshan groups (BGMRGX, 1985; BGMRGZ, 1987; Figs. 2, 3, 4), which display a similar litho-stratigraphic succession of sandy-argillaceous metasedimentary rocks, along with volcaniclastic rocks, siliceous marble, red jasper and some mafic–ultramafic rocks (BGMRGX, 1985; BGMRGZ, 1987). Tuff layers within these groups yield zircon U-Pb ages of 842 ± 6 Ma, 832 ± 2 Ma and 840 ± 5 Ma (SHRIMP, Gao et al., 2010; LA-ICP-MS, Su et al., 2018a). Mafic-ultramafic assemblages in the southwest domain contain pillow basalt, gabbro, tholeiite, pyroxenite and peridotite, unlike equivalent sequences in the northeast and central domains of the Jiangnan Orogen that are dominated by ultramafic rocks. These assemblages have yielded ages in the range of 855–825 Ma (SHRIMP zircon U-Pb, 828 ± 7 Ma, Li et al. 1999; LA-ICP-MS zircon U-Pb, 841 ± 22 Ma, Zhou et al., 2007; LA-ICP-MS zircon U-Pb, 831 ± 6Ma and 827 ± 24Ma, Zhou et al., 2009; LA-ICP-MS zircon U-Pb, 829 ± 11 Ma, Zhao and Zhou, 2013; LA-ICP-MS zircon U–Pb, 855 ± 5 Ma, Yao et al., 2014a; LA-ICP-MS zircon U–Pb, 836 ± 44 Ma, Chen et al., 2017). Some high Mg diorites within the Sibao Group are dated at 837 ± 7 Ma (Chen et al., 2014; Wang et al., 2014b).

The Sibao and Fanjinshan groups are folded and sheared, and are unconformably overlain by the Danzhou and Xiajiang groups, respectively (BGMRGX, 1985; BGMRGZ, 1987; Figs. 2, 3, 4). The Danzhou group consists of mudstones and siltstones with lesser conglomerate, carbonate, basalt and volcaniclastic rocks, with depositional ages constrained at around 805 Ma to 730 Ma on the basis of tuff layers and youngest detrital zircons (Gao et al., 2014; Zhou et al., 2014 and references therein; Yang et al., 2015; Su et al., 2018a). For instance, zircon U-Pb ages of 803 ± 4 Ma and 764 ± 5 Ma have been determined for tuff layers in the Danzhou Group (Su et al., 2018a). The Xiajiang group display a lithostratigraphic composition of meta-sandstone, siltstone and slate, along with thin layers of carbonate, tuff and volcanics. The timing of deposition of the Xiajiang Group is constrained at around 815-810 Ma to 750 Ma according to age data of tuff layers and detrital zircons within the group (Gao et al., 2014; Wang et al., 2010). The Danzhou and Xiajiang groups are overlain by rocks of the upper Nanhua Basin (Fig. 2).

3.4 Ophiolitic mélanges

Two disrupted ophiolitic sequences occur within the Jiangnan Orogen along the Northeast Jiangxi and Shaoxing–Jiangshan fault zones (Fig. 3; Zhou et al., 1989; Shu et al., 2006; Yao et al., 2016b; Charvet, 2013). The former contains an older ophiolite (northeastern Jiangxi) dated at ca. 1000–960 Ma and a younger one (referred to as ‘south Anhui’ or ‘Fuchuan’) dated at ca. 830 Ma (whole rock Sm-Nd, SIMS and LA-ICP-MS Zircon U-Pb, Zhou et al., 1989; Chen et al., 1991; Li et al., 1994, 1997; Zhang et al., 2012b; 2013a; Wang et al., 2015a; Sun et al., 2018b). Ophiolite components of the Northeast Jiangxi and Fuchuan ophiolitic zones, including ultramafic suites, gabbro, pillow basalts and deep–sea sedimentary rocks, are well preserved and occur as structural blocks within a serpentinite matrix (Shu, 2012 and references there in; Zhang et al., 2012b, 2013a; Wang et al., 2015a;). Adakitic granite and mafic enclave-bearing plagiogranite occur within the Northeast Jiangxi ophiolite mélange, with the latter dated at 970 ± 21 Ma (SHRIMP zircon U-Pb) and has isotopic and chemical signatures indicative of derivation from a depleted mantle source (Li and Li, 2003; Gao et al., 2009). Both ophiolitic fragments along the Northeast Jiangxi and Fuchuan ophiolite zones are inferred to be supra-subduction zone type, possibly formed in a back-arc marginal sea (Shu et al., 1995, 2019; Zhang et al., 2012a; Sun et al., 2018b). Ophiolite components of the Shaoxing-Jiangshan ophiolitic fault zone are not well preserved, and include minor ultramafic-mafic suites (dunite, lherzolite, gabbro, pyroxinite and pillow basalt) dated at around 870–855 Ma sporadically occur within the eastern segment of the Shaoxing–Jiangshan fault zone, along with some deep-sea turbidities (Zhou and Zhu, 1992; Shu et al., 2006; Yao et al., 2016b).

A ca. 870–860 Ma ophiolitic mélange, consisting of mafic–ultramafic igneous rocks, chert, siliceous marble and ophicalcite within a matrix of phyllite, occurs along the east margin of the southwest domain (Yao et al., 2016a). The mélange contains oceanic exotic block and arc autochthonous block in a matrix of sandy and tuffaceous phyllite. The ophiolite is inferred to have been emplaced in a fore-arc setting (Yao et al., 2016a). In addition, N-MORB type meta-basalt dated at 860 ± 20 Ma and 838 ± 12 Ma have also been reported from localities within the Shuangqiaoshan and Lengjiaxi groups in the central domain and is interpreted as relic of back-arc or fore-arc oceanic crust (Zhang et al., 2013b; Yao et al., 2014b). High Mg pillow basalt occurs in the Fanjinshan Group of the southwest domain (Zhao and Zhou, 2013).

3.5 Age, character and distribution of granites

Neoproterozoic granitoids, including I- and S-types, occur within the Jiangnan Orogen (e.g. Guo et al., 1989, 1996; Li et al., 2003a; Wang et al., 2006; Zhao et al., 2013; Yao et al., 2014a, 2014b; Xin et al., 2017; Chen et al., 2018).

I-type granites dated at ca. 910–850 Ma have been identified in the southeast margin of the northeast domain (Ye et al., 2007; Yao et al., 2016b). A small I-type granite pluton, the Lantian pluton, dated at 821 ± 6 Ma occurs in the western central domain (Liu and Zhao, 2017). I-type granites have not yet been reported from other regions of the Jiangnan Orogen. Tourmaline-bearing leuco-granite, dated at 904 ± 5 Ma, also occur as enclaves within serpentinite in the Northeast Jiangxi suture zone (Wang et al., 2019).

Voluminous S-type granites, exposed over approximately 7000 km^2, outcrop in the central (Xucun, Xiuning, Jiuling and Meixian plutons) and southwest (Fanjingshan, Yuanbaoshan, Bendong and Sanfang plutons) domains of the Jiangnan Orogen, and yield emplacement ages of ca. 845–815 Ma and ca. 835–820 Ma, respectively (Li et al., 1999, 2003; Wang et al., 2006; Xue et al., 2010; Zhao et al., 2013; Deng et al., 2018; Wei et al., 2018). The granites intruded into the lower part of the Shuangqiaoshan, Sibao and their equivalent groups (Fig. 3; Shu, 2012; Yao et al., 2014a; Sun et al., 2017). The granites all contain peraluminous minerals such as muscovite, and display high ACNK values (e.g. Li et al., 2003a; Zhao et al., 2013; Yao et al., 2014a; Chen et al., 2018). The granites in the southwest domain contain higher SiO2 compositions, as well as a higher proportion of older inherited grains (Fig. 6) (Li et al., 2003a; Wang et al., 2006; Yao et al., 2014a) than those in the central domain. Likewise, the granites in the central domain show a transitional character between S-type and I-type affinities (Fig. 7; Wu et al., 2006; Xin et al., 2017). Amphibole and dioritic enclaves occur in the granites in the central domain as well, but are absent from those of the southwest domain (Sun et al., 2017). Moreover, the majority of zircons from S-type granites in the central Jiangnan Orogen show positive Hf values and low δ^{18}O variations as compared to those than those from the southwest domain (Figs. 6, 8; Zhao et al., 2011; Wang et al., 2013d).

3.6 Deformation and structural features

The Northeast Jiangxi and Shaoxing-Jiangshan fault zones constitute ductile shear zones (Charvet et al., 1996; Shu and Charvet, 1996). Microscopic shear indicators in the Northeast Jiangxi fault zone include pyrite pressure shadows, mica-fish tails, and dynamically recrystallized quartz aggregates (Shu and Charvet, 1996). Kinematic analysis indicates that the shear zone experienced polyphase ductile deformation, including southeastward thrusting at around 950–900 Ma and later sinistral strike-slip ductile shearing (Shu and Charvet, 1996; Xu et al., 2015). Whereas shear structures are less developed in the Shaoxing-Jiangshan fault zone. They have only been observed from the Sibao Group in the southwest domain of the Jiangnan Orogen and are characterized by top to east thrusting and strike slip motion as inferred from asymmetric folds and crenulations, asymmetric σ-type porphyroclasts, asymmetric fabrics of feldspar and quartz porphyroclast, as well as blocks of shared basalts (Fig. 4). The timing of deformation has not yet been directly dated, but field relations and a regional unconformity suggest a varied timing of shearing across the orogen, at some time between 820-815 to 805 Ma. Extensive deformation observed in the Shuangxiwu and Shangxi groups within the Shaoxing-Jiangshan and Northeast Jiangxi fault zone is dated as early Paleozoic (Xu et al., 2015; Li et al., 2016, 2017), which likely overprinted and was possibly co-axial with an earlier Neoproterozoic fabric. S-type granitic plutons in the central and southwest domains also display gneissic textures. Elsewhere within the orogen, Precambrian ductile deformation structures are rarely observed and ill-defined.

3.7 Metamorphism

Lithostratigraphic sequences and ophiolitic mélanges of the Jiangnan Orogen are primarily metamorphosed to lower greenschist facies. Timing of this metamorphic event has not been directly dated. But given the field relations that cleavage planes developed within greenschist facies metamorphic rocks stop at regional unconformity (Fig. 3), it must occurred before regional unconformity and after formation of the stratigraphic units, likely at ca. 820-815 Ma, which is coeval to the deformation of the Jiangnan Orogen. High-pressure blueschists (0.9~1.3 GPa, 250–450 ℃) also occur as a lens in ophiolitic blocks at Xiwan within the northeast Jiangxi suture zone and are dated at around 866 Ma (K-Ar on glaucophane) (Shu et al., 1994; Gao et al, 1996), but the precise metamorphic process (P-T-t paths) and settings remains unknown. Notably, in areas within the Shaoxing-Jiangshan fault zone and the Cathaysia Block, amphibolite to lower granulite facies metamorphism at ca. 446 ± 5 have been reported and are correlated with Phanerozoic orogenic movements (Shu, 2012; Wang et al., 2017). These events overprint and hinder recognition of Neoproterozoic metamorphic events in the Jiangnan Orogen.

4. Age and nature of convergent margin successions and implications for crustal growth patterns

Field relations, along with petrological, geochronological, isotopic and chemical data from igneous and sedimentary units (Shuangxiwu, Lengjiaxi, Sibao and their equivalents) across the Jiangnan Orogen, are consistent with formation along one or more convergent plate margins between ca. 970 Ma to 820 Ma (Figs. 9, 10, 11, 12; e.g. Zhou et al., 2004, 2014; Li et al., 2009, 2016b; Wang et al., 2014b, 2016b; Zhang and Wang, 2016; Yao et al., 2016a; Cui et al., 2017; Zhang et al., 2012c; 2017). This marks an overall period of crustal growth within the orogen (Figs. 5, 6, 10, 13; e.g. Wang et al., 2013d, 2014b; Yao et al., 2013; 2015). Subduction polarity is inferred as northwest or west directed beneath the northeast-central and southwest Jiangnan Orogen, respectively, based on the ductile southeast-directed and east-directed compressional structures in the orogen (Figs. 3, 4; Shu and Charvet, 1996; Xu et al., 2015; Yao et al., et al., 2016a).

4.1 The juvenile Huaiyu arc, northeast domain of the Jiangnan Orogen

The volcanic rocks and their intrusive equivalents within the Shuangxiwu Group display consistent intra–oceanic magmatic arc geochemical features with enrichment in LILEs and depletion of HFSEs (Nb–Ta, Zr–Hf) and plot in the island arc field (Fig. 9; Ye et al., 2007; Chen et al., 2009; Li et al., 2009; Yao et al., 2014c, 2016b). Similar chemical signatures have been observed in the I-type intrusions within the group (Ye et al., 2007; Yao et al., 2016b). Whole rock Nd ($3 < \varepsilon Nd(t) < 10$) and Sr ($(^{87}Sr/^{86}Sr)_i <$

0.704) isotopic data for the volcanic suites of the Shuangxiwu Group indicate they were derived from a depleted mantle source with no obvious crustal contamination (Fig. 10), whereas whole rock O isotopes reveal traces of minor sea water alteration (Shen et al., 1992). Furthermore, zircon grains from the I-type bodies, along with the Shuangxiwu volcanic rocks, all yield positive εHf(t) values with model ages at 1.1–0.95 Ga (Fig. 5), and thus are indicative of a young juvenile source with no older crustal component. Whole rock Nd analyses yield similar results with model ages of 1.1–0.9 Ga (Li et al., 2009). Overall age data from the Shuangxiwu Group and intrusions display a single early Neoproterozoic age population at ca. 970–850 Ma and lack older xenocrysts (Fig. 5). Therefore, we conclude that the northeast domain consists of Neoproterozoic juvenile arc lithologies (Shuangxiwu Group), termed the Huaiyu arc. This is also consistent with the presence of ophiolites along boundaries of the domain (Li et al., 1999; Shu et al., 2006).

4.2 Convergent continental margin successions in the central and southwest Jiangnan domains

Field relations, age patterns, isotopic and chemical features across the central and southwest domains of the Jiangnan Orogen indicate a convergent continental margin setting extending from around 890–880 Ma to 820 Ma with a westward decrease in age (Figs. 5, 9, 10, 11, 12, 13).

Ca. 870–820 Ma igneous suites in both domains, mostly tholeiitic mafic-ultramafic rocks concentrated at ca. 830 Ma, along with minor intermediate–felsic lithologies and I-type granite concentrated at ca. 845 Ma, yield subduction related geochemical signatures with typical depletions in HFSEs, such as Nb, Ta and Ti (Fig. 5, 9; e.g., Zhou et al., 2004; Zhao and Zhou, 2013; Chen et al., 2014; Wang et al., 2014a; Yao et al., 2014a; Zhang and Wang, 2016). These lithologies mostly display higher initial $^{87}Sr/^{86}Sr$ values and variable but lower and mostly negative εNd(t) values (Fig. 10 and references therein), than the northeast domain, indicating input of older crustal components or subduction fluid and trench sediments in the arc magma source.

Crustal contamination is also inferred from relatively lower and varied zircon εHf(t) values (0 < εHf(t) < 10) of grains with ages close to timing of crystallization of the rock suites (Fig. 5; e.g. Zhang and Wang, 2016; Chen et al., 2017; Sun et al., 2017), as well as their varied model ages of 1.5–0.9 Ga (Fig. 5 and references therein). In addition, older inherited zircon grains within the rock suites from the two domains display varied Hf isotopes and a wide range of model ages from Archean to earliest Neoproterozoic (Fig. 5). These data indicate the presence of evolved older crustal components in these arc magmatic suites and are consistent with age patterns of the S-type granites in both domains (Fig. 6). A few basaltic layers, or boudins within the Lengjiaxi Group, display LREE depleted patterns and depleted Nd isotopes (5 < εHf(t) < 10) that are comparable to N-MORB type basalt (Fig. 9; Zhang et al., 2013b; Yao et al., 2014b), which possibly reflect relics of sea mounts from subducting oceanic crust. Zhang et al. (2013) also inferred a back-arc basin setting for the N-MORB type basalts. In addition, E-MORB type basaltic layers have also been observed within the Shuangqiaoshan Group in the southeast margin of the central domain and are suggested as related to formation of retro-arc basins (Sun et al., 2017).

Detrital zircon grains from sediments of the Shuangqiaoshan Group and its equivalents in the central domain are dominated by ages in the range 880–820 Ma, which are close to the age of sedimentation (Figs. 11, 12). Archean and Mesoproterozoic detritus only constitute some 15% of dated grains. In contrast, zircons from the Sibao and Fanjinshan groups in the southwest domain contain 45% Archean to Mesoproterozoic aged detritus and other 50% in the range ca. 880–820 Ma (Fig. 11). All sedimentary successions in the two domains plot in the convergent margin field (Fig. 12; Cawood et al., 2012), consistent with their reported arc related geochemical data (Wang et al., 2012a). However, the Sibao Group and its equivalent units, exposed in the central and southwest Jiangnan domains, have also been interpreted to have formed in a within plate setting based on similarity of age patterns between this unit and the overlying Danzhou groups (Yang et al., 2015), with the arc related geochemical signatures interpreted as inherited from earlier arc systems (Li et al., 2003a, 2008b). Locally in the southwest Jiangnan domain, age patterns of the Sibao and Danzhou groups are comparable, perhaps due to less developed retro-continental arc basins and arc systems, but overall data and relations of units above and below the unconformity across the orogen display variably distinctive characters (Figs. 11, 14; Wang et al., 2012a, 2014b; Yao et al., 2019). More importantly, the interpretation is also inconsistent with the regional unconformity between Jiangnan Orogen and overlying Nanhua Basin succession at around 815–805 Ma (Fig. 11, 14), deformation and metamorphism between ca. 820 to ca. 815–805 Ma, the associated switch in geochemical signatures from convergent margin to within-plate (Fig. 9; Shu, 2012; Yao et al., 2014b; Wang et al., 2012c), and the transition from juvenile to crustal isotopic signatures (Figs. 5, 13, 15).

The presence of Archean to Mesoproterozoic zircons, both as detritus in convergent margin sedimentary rocks and as xenocrysts within arc type mafic igneous suites in the central and southwest domains of the Jiangnan Orogen (Fig. 5, 11), suggest the two domains include an older crustal basement, consistent with the Archean and Paleoproterozoic Hf and Nd model ages (Figs. 5, 13). Moreover, significant older crustal derived detritus in the southwest domain suggests a possible less developed retro-continental arc basin as compared to the central domain, as is reflected in the discrimination diagram of depositional settings (Fig. 12). Thus, the central and southwest domains resemble a Cordilleran (Andean) type convergent continental margin, rather than the intra-oceanic setting of the northeast domain. The related sedimentation occurred at approximately 890–820 Ma in a retro-arc and/or fore-arc continental margin basin. The retro-arc and fore-arc sediments, along with continental arc igneous suites, ophiolitic mélanges, sea mounts and turbidite, were accreted during continental assembly and formed the Sibao, Shuanqiaoshan and their equivalent groups.

More than 75% detrital zircons within the ca. 880-820 Ma populations obtained from the Shuangqiaoshan and equivalents units in the central domain are juvenile (0 < εHf(t)) and are suggestive of significant crustal growth at this age range (Fig. 13), whereas the equivalent sedimentary units in the southwest domain (Sibao and Fanjingshan groups) contain a greater proportion of older grains, with only 55% of grains yielding ages close to the depositional age (Fig. 11). Consequently, crustal reworking at around 880–820 Ma was less important in the central domain, but significant in the southwest domain (Fig. 13 and references therein).

5. Geodynamic significance of S-type granites in the Jiangnan Orogen: product of accretionary orogenic belt

Neoproterozoic S-type granites occur in the central and southwest domains of the Jiangnan Orogen, but are absent in the northeast domain (Huaiyu Terrane) (Fig. 1). The voluminous S-type granitoids have been considered to be generated by partial melting of crust related to a mantle plume and associated regional extensional event (Li et al., 2003a, 2003b), or to have formed in a post-collisional setting following continental assembly of South China (Wang et al., 2006; Zhao and Cawood, 2012 and references therein; Zhao et al., 2013). Any model for genesis of S-type granites in the Jiangnan Orogen must account for the following: 1) they yield similar ages of ca. 835–815 Ma (Fig. 6), or possibly as early as 845 Ma (Deng et al., 2018); 2) zircon Hf and O isotopes indicate a juvenile crust source for the S-type granites in the central domain but a source involving more reworked crustal compositions for those in the southwest domain (Fig. 6, 8); 3) ages of S-type granites overlap with arc magmatic suites and ophiolites, as well as convergent margin sedimentation as young as ca. 820–815 Ma (Figs. 5, 6, 11; e.g. Zhang et al., 2012b, 2012c, 2015; Chen et al., 2014; Wang et al., 2014b, 2015a, 2016b); 4) whole rock Sr and Nd isotopes of the granites and arc igneous suites in the central domain are comparable, as are those in the southwest domain (Fig. 10).

The prerequisite of S-type granite generation is to have a metasedimentary source or at least a high enough proportion of sedimentary rocks to produce peraluminous compositions (e.g., Chappell and White, 1974; Ague and Brimhall, 1987; Collins, 1996), and to be buried to middle or lower crust depths prior to anataxis. Many studies prefer burial and anataxis of the sedimentary rocks to occur in a post-collisional setting after continent-continent collision such as the Miocene granites in the Himalayas (Barbarin, 1998). Li et al. (2003a) also suggested a plume rifting model to achieve anataxis of sediments that produced the S-type granites in the Jiangnan Orogen. However, S-type granites also occur in accretionary orogens and indeed were originally defined on the basis of their occurrence in the Terra Australis accretionary orogen in eastern Australia (Chappell and White, 1974; Chappell, 1994). In accretionary settings, their formation has been related to extension generated re-melting of back-arc and arc-trench detritus during kinematic readjustments along the convergent plate margin (Collins and Richards, 2008; Kemp et al., 2010; Cawood et al., 2011).

S-type granites and subduction zone magmatism in both the central and southwest domains are temporally and spatially coincident (Fig. 5, 6; e.g. Wang et al., 2006, 2014a; Zhou et al., 2004; Yao et al., 2014a; Chen et al., 2014, 2017), as well as with sediment accumulation in back-arc or fore-arc basin settings (e.g., Wang et al., 2012a, 2014b; Zhang et al., 2017; Su et al., 2018a; Yao et al., 2019). S-type granites in the central Jiangnan domain display some subduction related geochemical features similar to arc igneous suites and plot in the field of volcanic arc granite (Fig. 7; e.g. Wu et al., 2006; Sun et al., 2017; Xin et al., 2017). In contrast, those in the southwest domain display positive Rb, Cs anomalies and negative Sr, Ba, Zr, Hf anomalies that are similar to highly evolved granites (Fig. 7; Yao et al., 2014a). The majority of the granite samples in the central domain display low whole rock initial $^{87}Sr/^{86}Sr$ ratios (< 0.7085) and high εNd(t) values in the range of -0.2 ~ -3 (Fig. 10), which are comparable to arc igneous suites in the domain, similar to S-type granites reported from the New England region in east Australia (cf., Flood and Shaw, 1977; Shaw and Flood, 1981). The results also coincide with the mostly positive εHf(t) values and low $\delta^{18}O$ values (6 ~ 10) of zircon grains from these granites, suggesting partial melting of juvenile lithologies and addition of juvenile input to form these granites (Fig. 8; Kemp et al., 2009; Shaw and Flood, 2009; Shaw et al., 2011), consistent with their younger latest Mesoproterozoic average model ages (Fig. 6). The majority of the granite samples in the southwest domain display higher whole rock initial $^{87}Sr/^{86}Sr$ ratios (>0.707) and lower εNd(t) values (< –3) (Fig. 10), with peak Nd model ages constrained at ca. 1.85 Ga, and coincide with zircon Hf-O isotopes showing consistent crustal signatures, along with zircon Hf model ages concentrated at ca. 1.9 Ga (Fig. 6). The overall isotopic data of S-type granites in the southwest Jiangnan domain indicate partial melting of crustal components of various ages, but with an average age of Paleoproterozoic, and are comparable to isotopic signatures of those of the Terra Australis Orogen (Kemp et al., 2009).

Considering overall field and age relations, as well as chemical and isotopic data, we infer an accretionary orogenic setting for emplacement of S-type granites in the Jiangnan Orogen. Heat necessary for crustal melting to form the S-type granites within the two domains may reflect lithospheric extension within the upper plate of a subduction zone associated with slab roll back, in a similar scenario to that invoked in other accretionary orogens (Collins and Richards, 2008; Cawood et al., 2009, 2011). The S-type granites in the central domain were likely emplaced in a subduction zone, formed by partial melting of arc sedimentary rocks and fore-arc complexes, along with some magma mixing of mantle and crust derived magmas as indicated by dioritic enclaves within the granites (Fig. 4), similar to the Paleozoic New England accretionary belt (Cawood et al., 2011; Shaw et al., 2011). The melting in the southwest domain involved a more evolved metasedimentary source, perhaps similar to the Lachlan segment of the Terra Australis Orogen (Keay et al., 1997; Kemp et al., 2009), where the S-type granites formed in a back arc setting through melting of both continental and arc derived metasedimentary rocks.

6. An accretionary geodynamic model for the Jiangnan Orogen and constraints on final continental assembly

6.1 Accretionary history of the Jiangnan Orogen

Data and field relations outlined above indicate that the Jiangnan Orogen consists of three distinct tectonostratigraphic assemblages: the northeast domain (Huaiyu Terrane), the central domain, and the southwest domain, with each constituting part of an accretionary orogenic belt (Figs. 16 and 17). Based on these data, the following geodynamic model is proposed. Subduction in an intra-ocean setting of the Ancient South China Ocean between ca. 1000-820 Ma resulted in the 970–850 Ma island arc magmatism and related sedimentation forming the northeast domain (Fig. 16A), along with the ca. 1000– 825 Ma ophiolitic remnants that are preserved along the southeast and west margins of the domain. For the central and southwest domains, subduction of oceanic crust had commenced by 880–870 Ma, resulting in continental margin arc magmatism and sedimentation (Figs. 16B, 17). Ophiolitic mélanges occur along the northeastern and eastern margins of the central and southwest domains. The magmatic and sedimentary records indicate subduction continued within the two domains until around 820–815 Ma. Widespread S-type and minor I type granites were emplaced during the latter part of this history (i.e., mostly 835–815 Ma) (Fig. 16C–1, –2). Starting at 845 Ma, slab retreat triggered mantle wedge upwelling, providing thermal input for partial melting of convergent continental margin sedimentary rocks and/or fore-arc assemblages and led to S-type granite emplacement (Fig. 16C–1). Slab rollback also contributed to rapid continental growth in the central Jiangnan domain as inferred from isotopic signatures of various lithologies. The slab rollback process was immediately followed by the assembly of Yangtze and Cathaysia blocks with the domains of the intervening Jiangnan Orogen.

6.2 Constraints on timing of assembly of South China

Estimates for the timing of final assembly of the Yangtze and Cathaysia blocks along the Jiangnan Orogen vary from ca. 880 Ma to ca. 830 Ma (e.g. Li et al., 1999; 2007; Wang et al., 2006, 2014c; Shu, 2012 and references therein; Yao et al., 2014a; Zhao, 2015; Cui et a., 2017; Xia et al., 2017; Wang et al., 2019). But the overall character of, and relationship between, the rock units within the Jiangnan Orogen, indicate that convergent margin sedimentation and arc-trench assemblages range in age from 970 Ma to 820 Ma (Fig. 5; Fig. 11). In addition, accretion of arc-basin and continental terranes within Cathaysia to form a unified block occurred at around ca. 900 Ma (Wang et al., 2014c), but arc magmatism along the margin of the block continued from ca. 1.0 Ga to ca. 860 Ma, or even ca. 825 Ma (Shu et al., 2008; Zhao, 2015; Xia et al., 2017; Wang et al., 2018). Thus, age and duration of subduction system in the Jiangnan Orogen and Cathaysia Block are comparable and suggest that final continental assembly did not take place until at least ca. 820–815 Ma. The upper age limit on assembly of the South China Craton is provided by the regional unconformity at the base of the overlying Nanhua Basin, which occurred at ca. 825 Ma in the northeast domain and at ca. 815–805 Ma in the central and south domains (Gao et al., 2010, 2011; Yao et al., 2013, 2015). Furthermore, the ages of regional deformation and associated greenschist facies metamorphism in the central and southwest domains are constrained between ca. 820–815 Ma and ca. 810-805 Ma, and at some time before ca. 825 Ma in the northeast domain. Therefore, we suggest the final assembly of continental blocks of South China, including the domains within the Jiangnan Orogen, occurred between ca. 825–805 Ma. Notably, the assembly processes display variations across the Jiangnan Orogen, and those in the northeast (ca. 825 Ma) occurred before those in the central and southwest domains (ca. 820 Ma to 810-805 Ma), consistent with age and distribution of trench-arc-basin assemblages across the orogen. The final continental assembly of South China occurred in a short timing interval, unlike most collisional orogen (Dewey, 2005), and favors an accretionary model for the Jiangnan Orogen and a double-sided subduction model for South China, which resulted in 'soft collision' of arc and continental blocks (Zhao, 2015).

7. Neoproterozoic paleogeography of South China

Paleogeographic models for the position of South China in Rodinia include internal (Li et al., 2008b), external (e.g. Cawood et al., 2013, 2018; Yu et al., 2008; Wang et al., 2013e; Zhao et al., 2018a), and separate plate settings (Merdith et al., 2017). Differences between these models are largely based on the ages and characters of rock units in South China and India, to which South China is inferred to be joined in some of these models. There is a paucity of paleomagnetic data to adequately constrain the position of these blocks within Rodinia in the early Neoproterozoic.

Late Mesoproterozoic to middle Neoproterozoic belts in South China display an apparent overall northwestward decrease in age. Field relations and data indicate that the Jiangnan accretionary orogenic belt was active from around 970 Ma to 820–815 Ma. Isotopic and geochemical data from the Panxi-Hannan belt along western and northwest margins of the Yangtze Block provide evidence for subduction-related accretionary orogenic activity continuing to ca. 750 Ma and possibly ca. 700 Ma (e.g. Zhou et al., 2002; Dong et al., 2012, 2017; Wang et al., 2016c; Zhao et al., 2018b; Sun et al., 2019). Although some works, favor an extension, rather than a convergent setting for the belt during this time (e.g. Li et al., 2003b). Recent data also suggest that subduction and accretion in the Wuyi-Yunkai domain of the Cathaysia Block was active at ca. 1000–900 Ma, and those in the northern margin of Cathaysia continued to ca. 825 Ma (Shu et al., 2008; Zhang et al, 2012a; Wang et al., 2013e, 2014c; Xia et al., 2017). Fingerprints of Mesoproterozoic activity, including amphibolite facies metamorphism at ca. 1.3–1.0 Ga, have been reported from Hainan Island, southern Cathaysia (Wang et al., 2015b; Yao et al., 2017; Zhang et al., 2019). But the relationship of Hainan Island to the rest of South China at this time in unconstrained.

Polar wonder paths of South China and India at ca. 820–802 Ma are comparable (Niu JW et al., 2016), indicating the two blocks were connected at this time. A possible coeval paleopole for Australia has been reported, but with poorly constrained ages

(Niu JW et al., 2016 and references therein). It is not until the Ediacaran period that a close link between the South China Craton and Australia can be established, with comparable apparent polar wander paths (Yang et al., 2004; Jing et al., 2015). Thus, in terms of paleomagnetic data, both the external model and separate plate model are permissible. On the other hand, convergent margin deposition and magmatism ceased at ca. 820 Ma in the Jiangnan Orogen and as young as 750–700 Ma in the Panxi-Hannan belt, arguing against an internal position of South China within Rodinia. This conclusion is consistent with the general absence of late Mesoproterozoic detritus in units of the Jiangnan Orogen and Nanhua Basin (Fig. 11, 14). The overall detrital age patterns of the sedimentary rocks from South China, India and west Australia are similar (Cawood et al., 2018; Wen et al., 2018), and indicative of close spatial affinities of these blocks. The Panxi-Hannan belt on the margin of South China is coeval with the Seychelles belt in west India (e.g. Ashwal et al., 2013), indicative a close link between India and South China. Therefore, overall paleomagnetic and geological data favor a position for South China adjacent to northern Australia and India, as shown in Figure 18.

Mesoproterozoic metamorphism in Hainan Island can be correlated with the Rayner-Eastern Ghats and Albany-Fraser belts (Cawood et al., 2008; Dasgupta et al., 2013), suggesting the region was situated somewhere near eastern India and southwest Australia. Hainan is separated from mainland China and may not have become part of Cathaysia until the early Paleozoic (Xu et al., 2014b; Cawood et al., 2018). On the other hand, the Jiangnan Orogen and Yangtze Block were accreted to Cathaysia on the northern Rodinia margin at around ca. 820-805 Ma. Active plate boundaries continued to ca. 750 Ma along the Panxi-Hannan belt on the northern and western margins of South China.

8. Conclusion

1. The Jiangnan Orogen can be divided into three domains: the northeast (Huaiyu

terrane), central and southwest domains. The Shuangxiwu Group in the northeast domain formed in an intra-oceanic arc. The Shuangqiaoshan, Sibao and their equivalent groups in the central and southwest domains are metasedimentary dominated and were mainly sourced from a ca. 880–820 Ma continental magmatic arc system, with strata accumulating in arc related basins.

2. The S-type granites in the central and southwest domains of the Jiangnan Orogen, range from ca. 845–815 Ma. They were, emplaced in an accretionary convergent plate margin setting, prior to the final assembly of the South China Craton, rather than during plume rifting or post-continent collisional extension. The granites were triggered by slab roll back, which enabled melting the fore-arc and/or back-arc basin assemblages.

3. The Jiangnan Orogen is an accretionary orogenic belt. Assembly of the Yangtze and Cathaysia blocks was completed by ca. 815–805 Ma, followed by development of a continental extensional basin, namely the Nanhua Basin.

4. Limited paleomagnetic data and sedimentation records, along with rock relations and patterns across South China, suggest it occupied an external position on the periphery of Rodinia, between India and west Australia.

Acknowledgements

We thank the Major State Research Development Program of China (Grant No. 2016YFC0600202) for financial support, as well as financial support from National Natural Science Foundation of China (Nos. 41330208, 41572200 and 41190070) and State Key Laboratory for Mineral Deposits Research (Nanjing University) (ZZKT–201603). Peter A. Cawood acknowledges support from Australian Research Council grant FL160100168. The manuscript benefited from insightful reviews by Dr. Trond Slagstad and two anonymous reviewers.

References

Ague, J.J., Brimhall, G.H., 1987. Granites of the batholiths of California: Products of local assimilation and regional-scale crustal contamination: Geology 15, 63–66.

Ashwal, L.D., Solanki, A.M., Pandit, M.K., Corfu, F., Hendriks, B.W.H., Burke, K., Torsvik, T.H., 2013. Geochronology and geochemistry of Neoproterozoic Mt. Abu granitoids, NW India: regional correlation and implications for Rodinia paleogeography. Precambrian Research 236, 265–281.

Barbarin, B., 1998. A review of the relationships between granitoid types, their origins and their geodynamic environments. Lithos 46, 605–626.

BGMRGX (Bureau of Geology and Mineral Resources of Guangxi province), 1985. Regional Geology of Guangxi Autonomous Region. Geological Publishing House, Beijing, pp. 1–853 (in Chinese with English Abstract).

BGMRGZ (Bureau of Geology and Mineral Resources of Guizhou Province), 1987. Regional Geology of Guizhou Province. Geological Publishing House, Beijing, pp. 1–666 (in Chinese with English Abstract).

BGMRHN (Bureau of Geology and Mineral Resources of Hunan Province), 1988. Regional Geology of Hunan Province. Geological Publishing House, Beijing, pp. 6–664 (in Chinese with English Abstract).

BGMRJX (Bureau of Geology and mineral Resources Jiangxi Province). 1984. Regional Geology of Jiangxi Province. Geology Publishing House, Beijing, pp. 2–725 (In Chinese with English abstract).

BGMRZJ (Bureau of Geology and mineral Resources Jiangxi Province), 1989. Regional Geology of Jiangxi Province. Geology Publishing House, Beijing, 5–575 (In Chinese with English Abstract).

Cai, Y.F., Wang, Y.J., Cawood, P.A., Fan, W.M., Liu, H.C., Xing, X.W., Zhang, Y.Z., 2014. Neoproterozoic subduction along the Ailaoshan zone, South China: Geochronological and geochemical evidence from amphibolite. Precambrian Research 245, 13–28.

Cai, Y.F., Wang, Y.J., Cawood, P.A., Zhang, Y.Z., Zhang, A., 2015. Neoproterozoic crustal growth of the Southern Yangtze Block : Geochemical and zircon U-Pb geochronological and Lu–Hf isotopic evidence of Neoproterozoic diorite from the Ailaoshan zone. Precambrian Research 266, 137–149.

Cawood, P. A., 2005. Terra Australis Orogen: Rodinia breakup and development of the Pacific and Iapetus margins of Gondwana during the Neoproterozoic and Paleozoic. Earth–Science Reviews 69(3–4), 249–279.

Cawood, P. A., Kroner, A., Collins, W. J., Kusky, T. M., Mooney, W. D., Windley, B. F., 2009. Accretionary orogens through Earth history. Geological Society, London, Special Publications 318, 1–36.

Cawood, P. A., Leitch, E. C., Merle, R. E., Nemchin, A. A., 2011. Orogenesis without collision: Stabilizing the Terra Australis accretionary orogen, eastern Australia. Bulletin 123(11–12), 2240-2255.

Cawood, P.A., Hawkesworth, C.J., Dhuime, B., 2012. Detrital zircon record and tec-tonic setting. Geology 40 (10), 875–878.

Cawood, P. A., Hawkesworth, C. J., Dhuime, B., 2013a. The continental record and the generation of continental crust. Geological Society of America, Bulletin 125(1-2), 14-32.

Cawood, P.A., Wang, Y.J., Xu, Y.J., Zhao, G.C., 2013b. Locating South China in Rodinia and Gondwana: a fragment of Greater Indian Lithosphere? Geology 41(8), 903–906.

Cawood, P.A., Strachan, R.A., Pisarevsky, S.A., Gladkochub, D.P., Murphy, J.B., 2016. Linking collisional and accretionary orogens during Rodinia assembly and breakup: Implications for models of supercontinent cycles. Earth and Planetary Science Letters 449, 118–126.

Cawood, P.A., Zhao, G.C., Yao, J.L., Wang, W., Xu, Y.J., Wang, Y.J., 2018. Reconstructing South China in Phanerozoic and Precambrian supercontinents. Earth-Science Reviews 186, 173-194.

Chappell, B.W., White, A.J.R., 1974. Two contrasting granite types. Pacific Geology 8(1), 173–174.

Chappell, B.W., 1994. Lachlan and New England: Fold belts of contrasting magmatic and tectonic development. Journal and Proceedings of the Royal Society of New South Wales 127, 47–59.

Charvet, J., Shu, L.S., Shi, Y.S., Guo, L.Z., Faure, M., 1996. The building of south China: collision of Yangtze and Cathaysia blocks, problems and tentative answers. Journal of Southeast Asian Earth Sciences 13 (3–5), 223–235.

Charvet, J., 2013. The Neoproterozoic–early Paleozoic tectonic evolution of the South China Block: an overview. Journal of Asian Earth Sciences 74, 198-209.

Chen, B., Gu, H., Chen, Y., Sun, K., Chen, W., 2018. Lithium isotope behaviour during partial melting of metapelites from the Jiangnan Orogen, South China: Implications for the origin of REE tetrad effect of F–rich granite and associated rare–metal mineralization. Chemical Geology 483, 372–384.

Chen, J.F., Foland, K.A., Xing, F., Xu, X.S., Zhou, T.X., 1991. Magmatism along the southeast margin of the Yangtze Block: Precambrian collision of the Yangtze and Cathaysia Blocks of China. Geology 19, 815–818.

Chen, H., Ni, P., Chen, R.Y., Lv, Z.C., Pang, Z.S., Wang, G.G., Yuan, H.X., 2016. Chronology and geological significance of spillite-keratophyre in Pingshui Formation, northwest Zhejiang Province. Geology in China 43(2), 410-418 (in Chinese with English abstract).

Chen, Q., Sun, M., Zhao, G., Zhao, J., Zhu, W., Long, X., Wang, J. 2019. Episodic crustal growth and reworking of the Yudongzi terrane, South China: Constraints from the Archean TTGs and potassic granites and Paleoproterozoic amphibolites. Lithos, 1-18.

Chen, X, Wang, D., Wang, X.L., Gao, J.F., Shu, X.J., Zhou, J.C., Qi, L., 2014. Neoproterozoic chromite-bearing high-Mg diorites in the western part of the Jiangnan orogen, southern China: Geochemistry, petrogenesis and tectonic implications. Lithos 200–201, 35–48.

Chen, X., Wang, X. L., Wang, D., Shu, X. J., 2017. Contrasting mantle-crust melting processes within orogenic belts: Implications from two episodes of mafic magmatism in the western segment of the Neoproterozoic Jiangnan Orogen in South China. Precambrian Research 309, 123-137.

Chen, Z.H., Xing, G.F., Guo, K.Y., Dong, Y.G., Chen, R., Zeng, Y., Li, L.M., He, Z.Y., Zhao, L., 2009. Petrogenesis of the Pingshui keratophyre from Zhejiang: Zircon U–Pb age and Hf isotope constraints. Chinese Science Bulletin 54, 610–617.

Collins, W.J., 1996. S- and I-type granitoids of the eastern Lachlan fold belt: Products of three-component mixing. Royal Society of Edinburgh Transactions, Earth Sciences 88, 171–179.

Collins, W.J., 2002. Nature of extensional accretionary orogens. Tectonics 21, 1–12.

Collins, W.J., Richards, S.W., 2008. Geodynamic significance of S-type granites in circum-Pacific orogens. Geology 36, 559–562.

Cui, X., Zhu, W.B., Fitzsimons, I.C.W., He, J.W., Lu, Y.Z., Wang, X., Ge, R.F., Zheng, B.H., Wu, X.H.,

2015. U–Pb age and Hf isotope composition of detrital zircons from Neoproterozoic sedimentary units in southern Anhui Province, South China: Implications for the provenance, tectonic evolution and glacial history of the eastern Jiangnan Orogen. Precambrian Research 271, 65–82.

Cui, X., Zhu, W., Fitzsimons, I. C. W., Wang, X., Lu, Y., Wu, X., 2017. A possible transition from island arc to continental arc magmatism in the eastern Jiangnan Orogen, South China: Insights from a Neoproterozoic (870–860 Ma) gabbroic–dioritic complex near the Fuchuan ophiolite. Gondwana Research 46, 1-16.

Dasgupta, S., Bose, S.B., Das, K., 2013. Tectonic evolution of the Eastern Ghats Belt, India. Precambrian Research 227, 247–258.

Deng, T., Xu, D., Chi, G., Zhu, Y., Wang, Z., Chen, G., Li, Z., Zhang, J., Ye, T., Yu, D., 2018. Revisiting the ca. 845–820-Ma S-type granitic magmatism in the Jiangnan Orogen: new insights on the Neoproterozoic tectono-magmatic evolution of South China. International Geology Review, 1-21.

Dewey, J. F., 2005. "Orogeny can be very short." Proceedings of the National Academy of Sciences of the United States of America 102(43): 15286-15293.

Dong, S.W., Zhang, Y.Q., Gao, R., Su, J.B., Liu, M., Li, J.H., 2015. A possible buried Paleoproterozoic collisional orogen beneath central South China: Evidence from seismic-reflection profiling. Precambrian Research 264, 1–10.

Dong, Y., Liu, X., Santosh, M., Chen, Q., Zhang, X., Li, W., Chen, B., He, D., Zhang, G., 2012. Neoproterozoic accretionary tectonics along the northwestern margin of the Yangtze Block, China: constraints from zircon U–Pb geochronology and geochemistry. Precambrian Research 196, 247-274.

Dong, Y., Sun, S., Yang, Z., Liu, X., Zhang, F., Li, W., Chen, B., He, D., Zhang, G., 2017. Neoproterozoic subduction-accretionary tectonics of the South Qinling Belt, China. Precambrian Research, 293, 73-90.

Deng, T., Xu, D., Chi, G., Zhu, Y., Wang, Z., Chen, G., Li, Z.H., Zhang, J.L., Ye, T.W., Yu, D., 2018. Revisiting the ca. 845–820-Ma S-type granitic magmatism in the Jiangnan Orogen: new insights on the Neoproterozoic tectono-magmatic evolution of South China. International Geology Review, 1-21.

Flood, R. H., Shaw S. E., 1977. Two 'S-type' granite suites with low initial 87Sr/86Sr ratios from the New England Batholith, Australia. Contribution to Mineralogy Petrology 61, 163-173.

Gao, J., Klemd, R., Long, L.L., Xiong, X.M., Qian, Q., 2009. Adakitic signature formed by ractional crystallization: An interpretation for the Neo-Proterozoic meta-plagio granites of the NE Jiangxi ophiolitic mélange belt, South China. Lithos 110, 277-293.

Gao, L.Z., Yang, M.G., Ding, X.Z., Liu, Y.X., Liu, X., Ling, L.H., Zhang, C.H., 2008. SHRIMP U-Pb zircon dating of tuff in the Shuangqiaoshan and Heshangzhen groups in South China—constraints on the evolution of the Jiangnan Neoproterozoic orogenic belt. Geological Bulletin of China 27, 1744-1751(Chinese with English abstract).

Gao, L.Z., Dat C G, Liu Y X, Wang M, Wang X I-I, Chen J S, Ding X Z, Zhang C H, Cao Q, Liu J H., 2010. Zircon SHRIMP U-Pb dating of tuff bed of the Sibao Group in southeastern Guizhou-northern Guangxi area, China and its stratigraphic implication. Geological Bulletin of China 9(9), 1259-1267

Gao, L.Z., Chen, J., Ding, X.Z., Liu, Y.R., Zhang, C.H., Zhang, H., Liu, Y.X., Pang, W.H., Zhang, Y.H., 2011. Zircon SHRIMP U–Pb dating of the tuff bed of Lengjiaxi and Banxi groups, northeastern Hunan: constraints on the Wuling Movement. Geological Bulletin of China 30 (7), 1001–1008 (in Chinese with English Abstract).

Gao, L.Z., Chen, J.S., Dai, C.G., Ding, X.Z., Wang, X.H., Liu, Y.X., Wang, M., Zhang, H., 2014. SHRIMP zircon U-Pb dating of tuff in Fanjingshan Group and Xiajiang Group from Guizhou and Hunan Provinces and its stratigraphic implications. Geological Bulletin of China 33(7), 949-959.

Gao, S., Zhang, B.R., 1990. The discovery of Archean TTG gneisses in northern Yangtze craton and their implications. Earth Science 15, 675–679.

Greentree, M. R., Li, Z.X, Li, X.H, Wu, H.C, 2006. Late Mesoproterozoic to earliest Neoproterozoic basin record of the Sibao orogenesis in western South China and relationship to the assembly of Rodinia. Precambrian Research 151(1), 79–100.

Guo, L.Z., Shi, Y.S., Lu, H.F., Ma, R.S., Dong, H.G., Yang, S. F., 1989. The pre-Devonian tectonic patterns and evolution of South China. Journal of Southeast Asian Earth Science 3, 87–93.

Guo, L.Z., Lu, H.F., Shi, Y.S., Ma, R.S., Sun, Y., Shu, L.S., Jia, D., Zhang, Q.L., Faure, M., Charvet, J.,

1996. On the Meso-Neoproterozoic Jiangnan island arc: its kinematics and dynamics. Geological Journal of Universities 2(1), 1-13.

Guo, L., Gao, R., 2017. Potential-field evidence for the tectonic boundaries of the central and western Jiangnan belt in South China. Precambrian Research 309, 45-55.

Jing, X. Q., Yang, Z., Tong, Y., Han, Z., 2015. A revised paleomagnetic pole from the mid-Neoproterozoic Liantuo Formation in the Yangtze block and its paleogeographic implications. Precambrian Research 268, 194-211.

Keay, S., Collins, W.J., McCulloch, M.T., 1997. A three-component Sr-Nd isotopic mixing model for granitoid genesis, Lachlan fold belt, eastern Australia. Geology 25(4) 307–310.

Kemp, A. I. S., Hawkesworth, C. J., Collins, W. J., Gray, C. M., Blevin, P. L., 2009. Isotopic evidence for rapid continental growth in an extensional accretionary orogen: The Tasmanides, eastern Australia. Earth and Planetary Science Letters 284(3-4), 455-466.

Li, J.H., Dong, S.W., Zhang, Y.Q., Zhao, G.C., Johnston, S.T., Cui, J.J., Xin, Y.J., 2016a. New insights into Phanerozoic tectonics of south China: Part 1, polyphase deformation in the Jiuling and Lianyunshan domains of the central Jiangnan Orogen. Journal of Geophysical Research, Solid Earth 121, 3048–3080.

Li, J.H, Zhang, Y.Q, Zhao, G.C, Johnston, S. T., Dong, S.W, Koppers, A. A., Miggins, D.P., Sun, H.S., Wang, W.B., Xin, Y.J., 2017. New insights into Phanerozoic tectonics of South China: Early Paleozoic sinistral and Triassic dextral transpression in the east Wuyishan and Chencai domains, NE Cathaysia. Tectonics 36(5), 819–853.

Li, J.Y., Wang, X.L., Zhang, F.F., Zhou, X.H., Shu, X.J., 2016b. A rhythmic source change of the Neoproterozoic basement meta-sedimentary sequences in the Jiangnan Orogen: Implications for tectonic evolution on the southeastern margin of the Yangtze Block. Precambrian Research 280, 46–60.

Li, L.M., Sun, M., Wang, Y.J., Xing, G.F., Zhao, G.C., Lin, S.F., Xia, X.P., Chan, L.S., Zhang, F.F., Wong, J., 2011. U–Pb and Hf isotopic study of zircons from migmatised amphibolites in the Cathaysia Block: implications for the early Paleozoic peak tectonothermal event in Southeastern China. Gondwana Research 19, 191–201.

Li, L.M, Lin, S.F., Xing, G.F., Davis, D. W., Davis, W. J., Xiao, W., Yin, C., 2013. Geochemistry and tectonic implications of late Mesoproterozoic alkaline bimodal volcanic rocks from the Tieshajie Group in the southeastern Yangtze Block, South China. Precambrian Research 230, 179-192.

Li, L.M, Lin, S.F., Xing, G.F., Davis, D.W., Jiang, Y., Davise, W., Zhang, Y.J., 2016c. Ca. 830 Ma back-arc type volcanic rocks in the eastern part of the Jiangnan orogen: Implications for the Neoproterozoic tectonic evolution of South China Block. Precambrian Research 275, 209–224.

Li, W.X., Li, X.H., 2003. Adakitic granites within the NE Jiangxi ophiolites, South China: geochemical and Nd isotopic evidence. Precambrian Research 122, 29–44.

Li, W.X, Li, X.H, Li, Z.X, 2005. Neoproterozoic bimodal magmatism in the Cathaysia Block of South China and its tectonic significance. Precambrian Research 136(1), 51–66.

Li, X.H., Zhou, G.Q., Zhao, J.X., Fanning, C. M., Compston, W., 1994. SHRIMP ion microprobe zircon U-Pb age and Sm-Nd isotopic characteristics of the NE Jiangxi ophiolite and its tectonic implications. Chinese Journal of Geochemistry 13, 317-325.

Li, X.H., Zhao, J.X., McCulloch, M.T., Zhou, G.Q., Xing, F.M., 1997. Geochemical and Sm-Nd isotopic study of Neoproterozoic ophiolites from southeastern China: petrogenesis and tectonic implications. Precambrian Research 81, 129-144.

Li, X.H., Li, Z.X., Ge, W., Zhou, H., Li, W., Liu, Y., Wingate, M.T.D., 2003a. Neoproterozoic granitoids in South China: crustal melting above a mantle plume at ac. 825Ma? Precambrian Research 122, 45–83.

Li, X.H., Li, W.X., Li, Z.X., Liu, Y., 2008a. 850–790 Ma bimodal volcanic and intrusive rocks in northern Zhejiang, South China: A major episode of continental rift magmatism during the breakup of Rodinia. Lithos 102, 341–357.

Li, X.H, Li, W.X., Li, Z.X., Lo, C.H., Wang, J., Ye, M.F., Yang, Y.H., 2009. Amalgamation between the Yangtze and Cathaysia Blocks in South China: Constraints from SHRIMP U–Pb zircon ages, geochemistry and Nd–Hf isotopes of the Shuangxiwu volcanic rocks. Precambrian Research 174, 117–128.

Li, X. Y., Zheng, J. P., Xiong, Q., Zhou, X., Xiang, L., 2018. Triassic rejuvenation of unexposed Archean-Paleoproterozoic deep crust beneath the western Cathaysia block, South China.

Tectonophysics 724–725, 65-79.

Li, Z.X., Li, X.H., Kinny, P.D., Wang, J., 1999. The breakup of Rodinia: did it start witha mantle plume beneath South China? Earth and Planetary Science Letters 173,171–181.

Li, Z.X., Li, X.H., Zhou, H.W., Kinny, P.D., 2002. Grenvillian continental collision in South China: new SHRIMP U–Pb zircon results and implications for the configuration of Rodinia. Geology 30, 163–166.

Li, Z.X., Li, X.H., Kinny, P.D., Wang, J., Zhang, S., Zhou, H.W., 2003b. Geochronology of Neoproterozoic syn-rift magmatism in the Yangtze Craton, South China and correlations and correlations with other continents: evidence for a mantle super plume that broke up Rodinia. Precambrian Research 122, 85–109.

Li, Z.X., Wartho, J.A., Occhipinti, S., Zhang, C.L., Li, X.H., Wang, J., Bao, C.M., 2007. Early history of the eastern Sibao orogen (South China) during the assembly of Rodinia: new mica40Ar/39Ar dating and SHRIMP U–Pb detrital zircon provenance constraints. Precambrian Research 159, 79–94.

Li, Z.X., Bogdanova, S.V., Collins, A.S., Davidson, A., De Waele, B., Ernst, R.E., Fitzsimons, I.C.W., Fuck, R.A., Gladkochub, D.P., Jacobs, J., Karlstrom, K.E., Lu, S., Natapov, L.M., Pease, V., Pisarevsky, S.A., Thrane, K., Vernikovsky, V., 2008b. Assembly, configuration, and break-up history of Rodinia: a synthesis. Precambrian Research 160, 179–210.

Li, Z.X., Li, X.H., Li, W.X., Ding, S.J., 2008c. Was Cathaysia part of Proterozoic Laurentia? – new data from Hainan Island, south China. Terra Nova 20, 154–164.

Lin, M., Peng, S., Jiang, X., Polat, A., Kusky, T., Wang, Q., Deng, H., 2016. Geochemistry, petrogenesis and tectonic setting of Neoproterozoic mafic–ultramafic rocks from the western Jiangnan orogen, South China. Gondwana Research 35, 338-356.

Liu, H., Zhao, J. H., 2017. Neoproterozoic peraluminous granitoids in the Jiangnan Fold Belt: Implications for lithospheric differentiation and crustal growth. Precambrian Research 309, 152-165.

Ma, X., Yang, K., Li, X., Dai, C., Zhang, H., Zhou, Q., 2016. Neoproterozoic Jiangnan Orogeny in southeast Guizhou, South China: evidence from U–Pb ages for detrital zircons from the Sibao Group and Xiajiang Group. Canadian Journal of Earth Sciences 53(3), 219-230.

Merdith A.S., Collins, A.S., Williams, S.E., Pisarevsky, S., Foden, J.D., Archibald, D.B., Blades, Morgan.L., Alessio, B.L., Armistead, S., Plavsa, D., Clark, C., Müller, R.D., 2017. A full-plate global reconstruction of the Neoproterozoic. Gondwana Research 50, 84-134.

McDonough, W.F., Sun, S.S., 1995. Composition of the Earth. Chemical Geology 120, 223-253.

Niu, J.W, Li, Z.X., Zhu, W.G., 2016. Palaeomagnetism and geochronology of mid-Neoproterozoic Yanbian dykes, South China: implications for a c. 820–800 Ma true polar wander event and the reconstruction of Rodinia. Geological Society, London, Special Publications 424(1), P424-11.

Pan, C.C., Feng, Y.H., Xu, G.W., 1988. On the Proterozoic Cangshuipu Group and the Cangshuipu orogeny in South China. Geology of Jiangxi 2 (2), 138–145 (in Chinese with English abstract).

Pearce, J.A., 1982. Trace element characteristics of lavas from destructive plate boundaries, in: R.S. Thrope (Ed.), Andesites: Orogenic Andesites and Related Rocks. John Wiley and sons, Chichester, 525–548.

Pearce, J.A., Harris, N.B.W., Tindle, A.G., 1984. Trace element discrimination dia-grams for the tectonic interpretation of granitic rocks. Journal of Petrology 25,956–983.

Qiu, Y.M., Gao, S., McNaughton, N.J., Groves, D.I., Ling, W. 2000. First evidence of >3.2 Ga continental crust in the Yangtze craton of south China and its implications for Archean crustal evolution and Phanerozoic tectonics. Geology, 28 (1), 11–14.

Qi, L., Xu, Y.J., Cawood, P. A., Du, Y.S., 2018. Reconstructing Cryogenian to Ediacaran successions and paleogeography of the South China Block. Precambrian Research 314, 452-467.

Qi, L., Xu, Y.J., Cawood, P. A., Wang, W., Du, Y.S., 2019. Implications of 770 Ma Rhyolitic Tuffs, eastern South China Craton in constraining the tectonic setting of the Nanhua Basin. Lithos 324–325, 842-858.

Shaw, S.E., Flood, R.H., 1981, The New England Batholith, eastern Australia: Geochemical variations in time and space. Journal of Geophysical Research 86, 10530–10544.

Shaw, S.E., Flood, R.H., 2009, Zircon Hf isotopic evidence for mixing of crustal and silicic mantle-derived magmas in a zoned granite pluton, eastern Australia. Journal of Petrology 50, 147–168.

Shaw, S.E., Flood, R.H., Pearson, N.J., 2011. The New England Batholith of eastern Australia: Evidence of silicic magma mixing from zircon 176Hf/177Hf ratios. Lithos 126, 115–126.

Shen, W.Z., Zhang, B.T., Ling, H.F., Lai, M.Y., Yang, J.D., Tao, X.C., 1992. Nd, Sr and O Isotopic Study on Spilite-Keratophyre in Xiqiu,,Zhejiang Province, China. Acta Geologica Sinica (English edition) 66(2), 165-176 (In Chinese with English abstract).

Shu, L.S., Zhou, G.Q., Shi, Y.S., Yin, J., 1994. Study on the high pressure metamorphic blueschist and its Late Proterozoic age in the Eastern Jiangnan belt. Chinese Science Bulletin 39, 1200–1204.

Shu, L.S., Shi, Y.S., Guo, L.Z., Charvet. J., Sun, Y., 1995, The Late Proterozoic plate tectonics and collisional kinematics in the middle part of the Jiangnan belt. Nanjing: Nanjing University Publishing House, 1-174.

Shu, L.S., Charvet, J., 1996. Kinematics and geochronology of the Proterozoic Dongxiang - Shexian ductile shear zone: with HP metamorphism and ophiolitic melange (Jiangnan region, South China). Tectonophysics 267, 291–302.

Shu, L.S., Faure, M., Jioang, S.Y., Yang, Q., Wang Y.J., 2006. SHRIMP zircon U-Pb age, litho- and biostratigraphic analyses of the Huaiyu Domain in South China - Evidence for a Neoproterozoic orogen, not Late Paleozoic-Early Mesozoic collision. Episodes 29(4), 244-252.

Shu, L.S., 2006. Predevonian Tectonic Evolution of South China: from Cathaysian Block to Caledonian Period Folded Orogenic Belt. Geological Journal of China Universities 12(4), 418-431 (In Chinese with English abstract).

Shu, L.S., Deng, P., Yu, J.H., Wang, Y.B., Jiang, S.Y., 2008. The age and tectonic environment of the rhyolitic rocks on the western side of Wuyi Mountain, South China. Science in China (D) 38 (8), 950–959.

Shu, L.S., Faure, M., Yu, J.H., Jahn, B.M., 2011. Geochronological and geochemical features of the Cathaysia Block (South China): New evidence for the Neoproterozoic breakup of Rodinia. Precambrian Research 187 (3–4), 263–276.

Shu, L.S., 2012. An analysis of principal features of tectonic evolution in South China Block. Geological Bulletin of China 31(7), 1035-1053. (In Chinese with English abstract)

Shu, L.S., Jahn, B.M., Charvet, J., Santosh, M., Wang, B., Xu, X.S., Jiang, S. Y., 2014. Intraplate tectono-magmatism in the Cathaysia Block (South China): Evidence from stratigraphic, structural, geochemical and geochronological investigations. American Journal of Science 314, 154–186.

Shu, L., Wang, B., Cawood, P. A., Santosh, M., Xu, Z.Q., 2015. Early Paleozoic and early Mesozoic intraplate tectonic and magmatic events in the Cathaysia Block, South China. Tectonics 34, 1600-1621.

Su, H.M., Jiang, S.Y., Mao, J.W., Zhang, D.Y., Wu, X.K., Qin, H.F., 2018a. U-Pb ages and Lu-Hf isotopes of detrital zircons from sedimentary units across the Mid-Neoproterozoic unconformity in the western Jiangnan Orogen of South China and their tectonic implications. The Journal of Geology 126(2), 207-228.

Su, J.B., Dong, S.W., Zhang, Y.Q., Ma, L.C., Chen, X.H., Li, Y., 2018b. Formation process of mid-Neoproterozoic mafic rocks from the western Jiangnan Orogen, South China: insights from SHRIMP U–Pb dating and geochemical analysis. International Geology Review 60(3), 365-381.

Sun, J.J., Shu, L.S., Santosh, M., Wang, L.S., 2017. Neoproterozoic tectonic evolution of the Jiuling terrane in the central Jiangnan orogenic belt (South China): Constraints from magmatic suites. Precambrian Research 302, 279–297.

Sun, J.J., Shu, L.S., Santosh, M., Wang, L.S., 2018a. Precambrian crustal evolution of the central Jiangnan Orogen (South China): Evidence from detrital zircon U-Pb ages and Hf isotopic compositions of Neoproterozoic metasedimentary rocks. Precambrian Research 318, 1-24.

Sun, M., Chen, N., Zhao, G., Wilde, S. A., Ye, K., Guo, J., Chen. Y, Yuan, C. 2008. U–Pb zircon and Sm–Nd isotopic study of the Huangtuling granulite, Dabie–Sulu belt, China: Implication for the paleoproterozoic tectonic history of the Yangtze Craton. American Journal of Science 308(4), 469-483.

Sun, S.S., McDonough, W.F., 1989. Chemical and isotopic systematics of oceanic basalts: implication for mantle composition and processes. In: Saunder, A.D., Norry, M.J. (Eds.), Magmatism in the Ocean Basins. Geological Society, London, Special Publications 42, 313–345.

Sun, S.S, Dong, Y.P., Sun, Y.L., Cheng, C., Huang, X.X., Liu, X.M., 2019. Re-Os geochronology, O isotopes and mineral geochemistry of the Neoproterozoic Songshugou ultramafic massif in the Qinling Orogenic Belt, China. Gondwana Research 70, 71-87.

Sun, Z. M., Wang, X. L., Qi, L., Zhang, F. F., Wang, D., Li, J. Y., Yu, M.G., Shu, X. J., 2018b. Formation of the Neoproterozoic ophiolites in southern China: new constraints from trace element and PGE geochemistry and Os isotopes. Precambrian Research 309, 88-101.

Torsvik, T. H., 2003. The Rodinia jigsaw puzzle. Science 300(5624), 1379-1381.

Wang, D., Wang, X.L., Zhou, J.C., Shu, X.J., 2013a. Unraveling the Precambrian crustal evolution by Neoproterozoic conglomerates, Jiangnan orogen: U–Pb and Hf isotopes of detrital zircons. Precambrian Research 233, 223–236.

Wang, J., Li, X. H., Duan, T.Z., Liu, D. Y., Song, B., Li, Z.X., Gao, Y.H., 2003. Zircon SHRIMP U-Pb dating for the Cangshuipu volcanic rocks and its implications for the lower boundary age of the Nanhua strata in South China. Chinese Science Bulletin 48, 1663-1669.

Wang, J., Li, Z.X., 2003. History of Neoproterozoic rift basins in South China: implications for Rodinia break-up. Precambrian Research 122, 141–158.

Wang, J., Deng, Q., Wang, Z. J., 2013b. New evidence for sedimentary attributes and timing of the "Macaoyuan Group conglomerates" on the northern margin of the Yangtze block in southern China. Precambrian Research 235, 58-70.

Wang, J., Zhou, X., Deng, Q., Fu, X., Duan, T., Guo, X., 2015. Sedimentary successions and the onset of the Neoproterozoic Jiangnan sub-basin in the Nanhua rift, South China. International Journal of Earth Sciences 104(3), 521-539.

Wang, J.Q., Shu, L.S., Santosh, M., 2016a. Petrogenesis and tectonic evolution of Lianyunshan complex, South China: Insights on Neoproterozoic and late Mesozoic tectonic evolution of the central Jiangnan Orogen. Gondwana Research 39, 114–130.

Wang, J.Q, Shu, L.S, Santosh, M., 2017. U-Pb and Lu-Hf isotopes of detrital zircon grains from Neoproterozoic sedimentary rocks in the central Jiangnan Orogen, South China: Implications for Precambrian crustal evolution. Precambrian Research 294, 175-188.

Wang, J.Q., Shu, L.S, Yu, J.H., 2017. From the Neoproterozoic mafic rock to the Silurian high-grade metamorphic rock: evidence from zircon U-Pb geochronological, bulk-rock geochemical and mineral EPMA studies of Longyou garnet amphibolite in SE China. Journal of Asian Earth Sciences 141, 7-23.

Wang, L. J., Griffin, W. L., Yu, J. H., O'Reilly, S. Y., 2010. Precambrian crustal evolution of the

Yangtze Block tracked by detrital zircons from Neoproterozoic sedimentary rocks. Precambrian Research 177(1), 131-144.

Wang, W., Zhou, M.F., Yan, D.P., Li, J.W., 2012a. Depositional age, provenance, and tectonic setting of the Neoproterozoic Sibao Group, southeastern Yangtze Block, South China. Precambrian Research 192–195, 107–124.

Wang, W., Zhou, M. F., Yan, D. P., Li, L., Malpas, J., 2013c. Detrital zircon record of Neoproterozoic active-margin sedimentation in the eastern Jiangnan Orogen, South China. Precambrian Research 235, 1-19.

Wang, W., Zhao, J.H., Zhou, M.F., Yang, S.H., Chen, F.K., 2014a. Neoproterozoic Mafic-Ultramafic Intrusions from the Fanjingshan Region, South China: Implications for Subduction-Related Magmatism in the Jiangnan Fold Belt. The Journal of Geology 22(4) 455-473.

Wang, W., Zhou, M.F., Zhao, J.H., Pandit, M.K., Zheng, J.P., Liu, Z.R., 2016b. Neoproterozoic active continental margin in the southeastern Yangtze Block of South China: Evidence from the ca. 830–810 Ma sedimentary strata. Sedimentary Geology 342, 254–267.

Wang, W., Zhao, J.H., Zhou, M., Pandit, M.K., Zheng, J.P., 2018. Depositional age, provenance and tectonic setting of the Meso– and Neoproterozoic sequences in SE Yangtze Block, China: Implications on Proterozoic supercontinent reconstructions. Precambrian Research 309, 231–247.

Wang, X. C., Li, X. H., Li, Z. X., Li, Q. L., Tang, G. Q., Gao, Y. Y., Zhang, Q.R., Liu, Y., 2012b. Episodic Precambrian crust growth: evidence from U–Pb ages and Hf–O isotopes of zircon in the Nanhua Basin, central South China. Precambrian Research 222, 386-403.

Wang, X.L., Zhou, J.C., Qiu, J.S., Gao, J.F., 2004. Geochemistry of the Meso– to Neoproterozoic basic–acid rocks from Hunan Province, South China: implications for the evolution of the western Jiangnan orogen. Precambrian Research 135, 79–103.

Wang, X.L., Zhou, J.C., Qiu, J.S., Zhang, W.L., Liu, X.M., Zhang, G.L., 2006. LA-ICP-MS U–Pb zircon geochronology of the Neoproterozoic igneous rocks from Northern Guangxi Province, South China: implications for the tectonic evolution. Precambrian Research 145, 111–130.

Wang, X.L., Zhou, J.C., Griffin, W.L., Wang, R.C., Qiu, J.S., O'Reilly, S.Y., Xu, X.S., Liu, X.M., Zhang, G.L., 2007. Detrital zircon geochronology of Precambrian basement sequences in the

Jiangnan orogen: Dating the assembly of the Yangtze and Cathaysia Blocks. Precambrian Research 159, 117–131.

Wang, X.L., Zhao, G.C., Zhou, J.C., Liu, Y.S., Hu, J., 2008b. Geochronology and Hf isotopes of zircon from volcanic rocks of the Shuangqiaoshan Group South China: implications for the Neoproterozoic tectonic evolution of the eastern Jiangnan orogen. Gondwana Research 18, 355–367.

Wang, X.L., Shu, L.S., Xing, G.F., Zhou, J.C., Tang, M., Shu, X.J., Qi, L., Hu, Y.H., 2012c. Post-orogenic extension in the eastern part of the Jiangnan Orogenic belt: evidence from ca 800–760 Ma volcanic rocks. Precambrian Research 222–223, 404–423.

Wang, X. L., Zhou, J. C., Wan, Y. S., Kitajima, K., Wang, D., Bonamici, C., Qiu, J.S., Sun, T., 2013d. Magmatic evolution and crustal recycling for Neoproterozoic strongly peraluminous granitoids from southern China: Hf and O isotopes in zircon. Earth and Planetary Science Letters 366, 71-82.

Wang, X.L., Zhou, J.C., Griffin, W.L, Zhao GC, Yu JH, Qiu, J.S., Zhang, Y.J., Xing, G.F., 2014b. Geochemical zonation across a Neoproterozoic orogenic belt: Isotopic evidence from granitoids and metasedimentary rocks of the Jiangnan orogen, China. Precambrian Research 242, 154– 171.

Wang, X. S., Gao, J., Klemd, R., Jiang, T., Zhai, Q. G., Xiao, X. C., Liang, X., Q., 2015a. Early Neoproterozoic multiple arc–back-arc system formation during subduction-accretion processes between the Yangtze and Cathaysia blocks: new constraints from the suprasubduction zone NE Jiangxi ophiolite (South China). Lithos 236–237, 90–105.

Wang, X.S, Gao, J., Klemd, R., Jiang, T., Zhai, Q.G, Li, J.L, Liang, X.Q., 2019. From arc accretion to continental collision in the eastern Jiangnan Orogen: Evidence from two phases of S–type granites. Precambrian Research, 199–211.

Wang, Y.J., Zhang, A.M., Cawood, P.A., Fan, W.M., Xu, J.F., Zhang, G.W., Zhang, Y.Z., 2013e. Geochronological, geochemical and Nd-Hf-Os isotopic fingerprinting of an early Neoproterozoic arc-back-arc system in South China and its accretionary assembly along the margin of Rodinia. Precambrian Research 231, 343–371.

Wang, Y.J, Fan, W.M, Zhang, G.W., Zhang, Y.Z., 2013f. Phanerozoic tectonics of the South China Block: key observations and controversies. Gondwana Research 23(4), 1273-1305.

Wang, Y.J., Zhang, Y.Z., Fan, W.M., Geng, H.Y., Zou, H.P., Bi, X.W., 2014c. Early Neoproterozoic accretionary assemblage in the Cathaysia block: geochronological, Lu–Hf isotopic and geochemical evidence from granitoid gneisses. Precambrian Research 249, 144–161.

Wang, Y. J., Zhou, Y. Z., Cai, Y. F., Liu, H.C., Zhang, Y.Z., Fan, W.M., 2016c. Geochronological and geochemical constraints on the petrogenesis of the Ailaoshan granitic and migmatite rocks and its implications on Neoproterozoic subduction along the SW Yangtze Block. Precambrian Research 283, 106-124.

Wang, Y.J., Gan, C.S., Tan, Q.L., Zhang, Y.Z., He, H.Y., Xin, Q., Zhang, Y.H., 2018. Early Neoproterozoic (~840 Ma) slab window in South China: Key magmatic records in the Chencai Complex. Precambrian Research 314, 434–451.

Wang, Z.L, Xu, D.R., Hu, G.C, Yu, L.L, Wu, C.J, Zhang, Z.C, Cai, J.X., Shan, Q., Hou, M.Z., Chen, H.Y., 2015b. Detrital zircon U–Pb ages of the Proterozoic metaclastic-sedimentary rocks in Hainan Province of South China: New constraints on the depositional time, source area, and tectonic setting of the Shilu Fe–Co–Cu ore district. Journal of Asian Earth Sciences 113, 1143-1161.

Wei, S. D., Liu, H., Zhao, J. H., 2018. Tectonic evolution of the western Jiangnan Orogen: Constraints from the Neoproterozoic igneous rocks in the Fanjingshan region, South China. Precambrian Research 318 (2018) 89–102.

Windley, B. F., 1992. Proterozoic collisional and accretionary orogens. In: CONDIE, K. C. (ed.) Proterozoic Crustal Evolution. Developments in Precambrian Geology 10, 419–446.

Wood, D.A., 1980. The application of a Th–Hf–Ta diagram to problems of tecto-magmatic classification and to establishing the nature of crustal contamination of basaltic lavas of the British Tertiary volcanic province. Earth Planet Science Letters 50, 11–30.

Wu, R.X., Zheng, Y.F., Wu, Y.B., Zhao, Z.F., Zhang, S.B., Liu, X.M., Wu, F.Y. 2006. Reworking of juvenile crust: Element and isotope evidence from Neoproterozoic granodiorite in South China. Precambrian Research 146, 179–212.

Wu, Y.B., Gao, S., Gong, H.J., Xiang, H., Jiao, W.F., Yang, S.H., 2009. Zircon U–Pb age, trace element and Hf isotope composition of Kongling terrane in the Yangtze craton: refining the timing of Paleoproterozoic high–grade metamorphism. Journal of Metamorphic Geology 27, 461–477.

Xia, Y., Xu, X., Niu, Y., Liu, L., 2017. Neoproterozoic amalgamation between Yangtze and Cathaysia blocks: The magmatism in various tectonic settings and continent-arc-continent collision. Precambrian Research 309, 56-87.

Xiao, W.J, Windley, B. F., Hao, J., Zhai, M.G., 2003. Accretion leading to collision and the Permian Solonker suture, Inner Mongolia, China: Termination of the Central Asian Orogenic Belt. Tectonics 22, 1069, doi:10.1029/2002TC001484.

Xiao, W., Windley, B. F., Sun, S., Li, J., Huang, B., Han, C., Yuan, C., Sun, M., Chen, H., 2015. A tale of amalgamation of three Permo-Triassic collage systems in Central Asia: oroclines, sutures, and terminal accretion. Annual review of earth and planetary sciences 43, 477-507.

Xin, Y., Li, J., Dong, S., Zhang, Y., Wang, W., Sun, H., 2017. Neoproterozoic post-collisional extension of the central Jiangnan Orogen: Geochemical, geochronological, and Lu-Hf isotopic constraints from the ca. 820–800 Ma magmatic rocks. Precambrian Research 294, 91-110.

Xu, X.B., Xue, D.J., Li, Y., Hu, P., Chen, N.S., 2014a. Neoproterozoic sequences along the Dexing–Huangshan fault zone in the eastern Jiangnan orogen, South China: Geochronological and geochemical constrains. Gondwana Research 25, 368–382.

Xu, X.B., Li, Y., Tang, S., Xue, D.J., Zhang, Z.J., 2015. Neoproterozoic to Early Paleozoic polyorogenic deformation in the southeastern margin of the Yangtze Block: Constraints from structural analysis and 40Ar/39Ar geochronology. Journal of Asian Earth Sciences 98, 141-151.

Xu, Y., Cawood, P. A., Du, Y., Zhong, Z., Hughes, N. C., 2014b. Terminal suturing of Gondwana along the southern margin of South China Craton: Evidence from detrital zircon U- Pb ages and Hf isotopes in Cambrian and Ordovician strata, Hainan Island. Tectonics 33(12), 2490-2504.

Xue, H., Ma, F., Song, Y., Xie, Y., 2010, Geochronology and geochemisty of the Neoproterozoic granitoid association from eastern segment of the Jiangnan orogen, China Constraints on the timing and process of amalgamation between the Yangtze and Cathaysia blocks: Acta Petrologica Sinica 26, 3215–3244. (in Chinese with English abstract).

Yan, C.L, Shu, L.S., Santosh, M., Yao, J.L., Li, J.Y., Li, C., 2015. The Precambrian tectonic evolution of the western Jiangnan Orogen and western Cathaysia Block: Evidence from detrital zircon age spectra and geochemistry of clastic rocks. Precambrian Research 268, 33-60.

Yang, C., Li, X. H., Wang, X. C., Lan, Z., 2015. Mid-Neoproterozoic angular unconformity in the Yangtze Block revisited: Insights from detrital zircon U–Pb age and Hf–O isotopes. Precambrian Research 266, 165-178.

Yang, Z.Y., Sun, Z.M., Yang, T.S., Pei, J.L., 2004. A long connection (750-380 Ma) between South China and Australia: paleomagnetic constraints. Earth and Planetary Science Letters 220(3-4), 423-434.

Yao, J.L., Shu, L.S., Santosh, M., 2011. Detrital zircon U–Pb geochronology, Hf-isotopes and geochemistry — new clues for the Precambrian crustal evolution of Cathaysia Block, South China. Gondwana Research 20, 553–567.

Yao, J.L., Shu, L.S., Santosh, M., Li, J.Y. 2013. Geochronology and Hf isotope of detrital zircons from Precambrian sequences in the eastern Jiangnan Orogen: Constraining the assembly of Yangtze and Cathaysia Blocks in South China. Journal of Asian Earth Science 74, 225–243.

Yao, J.L, Shu, L.S., Santosh, M., Zhao, G.C., 2014a. Neoproterozoic arc-related mafic-ultramafic rocks and syn-collision granite from the western segment of the Jiangnan Orogen, South China: constraints on the Neoproterozoic assembly of the Yangtze and Cathaysia Blocks. Precambrian Research 243, 39-62.

Yao, J.L., Shu, L.S., Santosh, M., 2014b. Neoproterozoic arc-trench system and breakup of the South China Craton: constraints from N-MORB type and arc-related mafic rocks, and anorogenic granite in the Jiangnan orogenic belt. Precambrian Research 247, 187–207.

Yao, J.L., Shu, L.S., Santosh, M., Xu, Z.Q., 2014c. Palaeozoic metamorphism of the Neoproterozoic basement in NE Cathaysia: zircon U–Pb ages, Hf isotope and whole-rock geochemistry from the Chencai Group. Journal of the Geological Society, London 171, 281–297.

Yao, J. L., Shu, L. S., Santosh, M., Li, J. Y., 2015. Neoproterozoic arc-related andesite and orogeny-related unconformity in the eastern Jiangnan orogenic belt: constraints on the assembly of the Yangtze and Cathaysia blocks in South China. Precambrian Research 262, 84–100.

Yao, J.L, Cawood, P.A., Shu, L.S., Li, J.Y., 2016a. An Early Neoproterozoic Accretionary Prism Ophiolitic Mélange from the Western Jiangnan Orogenic Belt, South China. The Journal of Geology 124 (5), 587-601.

Yao, J. L., Shu, L. S., Cawood, P. A., Li, J. Y., 2016b. Delineating and characterizing the boundary of the Cathaysia block and the Jiangnan orogenic belt in South China. Precambrian Research 275, 265–277.

Yao, J. L., Shu, L. S., Cawood, P. A., Li, J. Y., 2017. Constraining timing and tectonic implications of Neoproterozoic metamorphic event in the Cathaysia Block, South China. Precambrian Research 293, 1–12.

Yao, W., Li, Z. X., Li, W. X., Li, X. H., 2017. Proterozoic tectonics of Hainan Island in supercontinent cycles: New insights from geochronological and isotopic results. Precambrian Research 290, 86-100.

Ye, M.F., Li, X.H., Li, W.X., Liu, Y., Li, Z.X., 2007. SHRIMP zircon U–Pb geochronological and whole-rock geochemical evidence for an early Neoproterozoic Sibaoan magmatic arc along the southeastern margin of the Yangtze Block. Gondwana Research 12, 144–156.

Yin, C., Lin, S., Davis, D. W., Xing, G., Davis, W. J., Cheng, G., Xiao, W., Li, L., 2013. Tectonic evolution of the southeastern margin of the Yangtze Block: Constraints from SHRIMP U-Pb and LA-ICP-MS Hf isotopic studies of zircon from the eastern Jiangnan Orogenic Belt and implications for the tectonic interpretation of South China. Precambrian Research 236, 145-156.

Yu, J.-H., O'Reilly, S.Y., Wang, L., Griffin, W.L., Zhang, M., Wang, R., Jiang, S., Shu, L., 2008. Where was South China in the Rodinia supercontinent? evidence from U-Pb geochronology and Hf isotopes of detrital zircons. Precambrian Research 164 (1–2), 1–15.

Yu, J.H., Wang, L.J., O'Reilly, S.Y., Griffin, W.L., Zhang, M., Li, C.Z., Shu, L.S., 2009. A Paleoproterozoic orogeny recorded in a long-lived cratonic remnant (Wuyishan terrane), eastern Cathaysia Block, China. Precambrian Research 174, 347-363.

Zhang, A.M., Wang, Y.J., Fan, W.M., Zhang, Y.Z., Yang, J., 2012a. Earliest Neoproterozoic (ca. 1.0 Ga) arc–back-arc basin nature along the northern Yunkai Domain of the Cathaysia Block: Geochronological and geochemical evidence from the metabasite. Precambrian Research 220–221, 217–233.

Zhang, B.T., Ling, H.F., Shen,W.Z., Liu, J.S., Yang, J.D., Tao, X.C., 1990. Sm–Nd isochronic age of spilite-keratophyre of Shuangxiwu Group in Xiqiu, Shaoxing, Zhejiang Province. Journal of

Nanjing University (Earth Science) 2, 9–14 (in Chinese with English Abstract).

Zhang, C.L, Santosh, M., Zou, H.B, Li, H.K, Huang, W., 2013a. The Fuchuan ophiolite in Jiangnan Orogen: Geochemistry, zircon U-Pb geochronology, Hf isotope and implications for the Neoproterozoic assembly of South China. Lithos 179, 263-274.

Zhang, F.F, Wang, X.L, Wang, D., Yu, J.H, Zhou, X.Y, Sun, Z.M, 2017. Neoproterozoic backarc basin on the southeastern margin of the Yangtze block during Rodinia assembly: New evidence from provenance of detrital zircons and geochemistry of mafic rocks. Geological Society of America Bulletin, 904-919.

Zhang, F. F., Wang, X. L., Sun, Z. M., Chen, X., Zhou, X. H., Yang, T., 2018. Geochemistry and zircon-apatite U-Pb geochronology of mafic dykes in the Shuangxiwu area: Constraints on the initiation of Neoproterozoic rifting in South China. Precambrian Research 309, 138–151.

Zhang, G.W., Guo, A.L., Wang, Y.J., Li, S.Z., Dong, Y.P., Liu, S.F., He, D.F., Cheng, S.Y., Lu, R.K., Yao, A.P., 2013b. Tectonics of South China Continent and its implications. Science in China (Earth Sciences) 56(11), 1804–1828.

Zhang, H., Gao, L.Z., Li, T.D., Geng, S.F., Liu, Y.X., Ding, X.Z., Shi, Z.G., 2015. SHRIMP zircon U-Pb dating of the Luojiamen Formation in western Zhejiang Province and its geological implications. Geological Bulletin of China 34(2/3), 447-455.

Zhang, S.B., Zheng, Y.F., Wu, Y.B., Zhao, Z.F., Gao, S., Wu, F.Y., 2006. Zircon U–Pb age and Hf isotope evidence for 3.8 Ga crustal remnant and episodic reworking of Archean crust in South China. Earth and Planetary Science Letters 252, 56–71.

Zhang, S.B., Wu, F.Y., Zheng, Y.F., 2012b. Neoproterozoic continental accretion in South China: Geochemical evidence from the Fuchuan ophiolite in the Jiangnan orogeny. Precambrian Research 220– 221, 45– 64.

Zhang, Y.Z, Wang, Y.J, Fan, W.M, Zhang, A.M, Ma, L.Y., 2012c. Geochronological and geochemical constraints on the metasomatised source for the Neoproterozoic (~825 Ma) high-mg volcanic rocks from the Cangshuipu area (Hunan Province) along the Jiangnan domain and their tectonic implications. Precambrian Research 220–221, 139-157.

Zhang, Y.Z, Wang, Y.J, Geng, H.Y, Zhang, Y.H, Fan, W.M, Zhong, H., 2013c. Early Neoproterozoic

(~850 Ma) back-arc basin in the Central Jiangnan Orogen (Eastern South China): Geochronological and petrogenetic constraints from meta-basalts. Precambrian Research 231, 325-342.

Zhang, Y.Z., Wang, Y.J., Zhang, Y.H., Zhang, A.M., 2015. Neoproterozoic assembly of the Yangtze and Cathaysia blocks: Evidence from the Cangshuipu Group and associated rocks along the Central Jiangnan Orogen, South China. Precambrian Research 269, 18–30.

Zhang, Y.Z., Wang, Y.J., 2016. Early Neoproterozoic (~840 Ma) arc magmatism: Geochronological and geochemical constraints on the metabasites in the Central Jiangnan Orogen. Precambrian Research 275, 1–17.

Zhang, L.M, Zhang, Y.Z, Cui, X., Cawood, P.A., Wang, Y.J, Zhang, A.M., 2019. Mesoproterozoic rift setting of SW Hainan: Evidence from the gneissic granites and metasedimentary rocks. Precambrian Research, 69–87.

Zhao, G.C., Cawood, P.A., 1999. Tectonothermal evolution of the Mayuan assemblage in the Cathaysia Block: implications for Neoproterozoic collision-related assembly of the South China craton. American Journal of Science 299, 309–339.

Zhao, G., Cawood, P. A., Wilde, S. A., Sun, M., 2002. Review of global 2.1–1.8 Ga orogens: implications for a pre-Rodinia supercontinent. Earth-Science Reviews 59(1-4), 125-162.

Zhao, G.C., Cawood, P.A., 2012. Precambrian Geology of China. Precambrian Research 222–223, 13–54.

Zhao, G. C., 2015. Jiangnan orogen in South China: developing from divergent double subduction. Gondwana Research 27, 1173–1180.

Zhao, G., Wang, Y., Huang, B., Dong, Y., Li, S., Zhang, G., Yu, S., 2018a. Geological reconstructions of the East Asian blocks: From the breakup of Rodinia to the assembly of Pangea. Earth-Science Reviews, doi.org/10.1016/j.earscirev.2018.10.003.

Zhao, J.H., Zhou, M.F., Yan, D.P., Zheng, J.P., Li, J.W., 2011. Reappraisal of the ages of Neoproterozoic strata in South China: no connection with the Grenvillian orogeny. Geology 39, 299–302.

Zhao, J.H., Zhou, M.F., 2013. Neoproterozoic high-Mg basalts formed by melting of ambient mantle in South China. Precambrian Research, 233, 193– 205.

Zhao, J.H., Zhou, M.F., Zhen, J.P., 2013. Constraints from zircon U–Pb ages, O and Hf isotopic compositions on the origin of Neoproterozoic peraluminous granitoids from the Jiangnan Fold Belt, South China. Contrib Mineral Petrol 166, 1505–1519.

Zhao, J. H., Li, Q. W., Liu, H., Wang, W., 2018b. Neoproterozoic magmatism in the western and northern margins of the Yangtze Block (South China) controlled by slab subduction and subduction-transform-edge-propagator. Earth-Science Reviews 187, 1-18.

Zhao, X.F., Zhou, M.F., Li, J.W., Wu, F., 2008. Association of Neoproterozoic A- and I-type granites in South China: Implications for generation of A-type granites in a subduction-related environment. Chemical Geology 257(1), 1-15.

Zhao, X.F., Zhou, M.F., Li, J.W., Sun, M., Gao, J., Sun, W.H., Yang, J.H., 2010. Late Paleoproterozoic to early Mesoproterozoic Dongchuan Group in Yunnan, SW China: Implications for tectonic evolution of the Yangtze Block. Precambrian Research 182(1), 57-69.

Zheng, J. P., Griffin, W. L., Li, L. S., O'Reilly, S. Y., Pearson, N. J., Tang, H. Y., Liu, G.L., Zhao, J.H., Yu, C.M., Su, Y. P., 2011. Highly evolved Archean basement beneath the western Cathaysia Block, south China. Geochimica et Cosmochimica Acta, 75(1), 242-255.

Zheng, J., Griffin, W. L., Oreilly, S. Y., Zhang, M., Pearson, N. J., Pan, Y. 2006. Widespread Archean basement beneath the Yangtze craton. Geology 34(6), 417-420.

Zheng, Y.F., Zhang, S.B., Zhao, Z.F., Wu, Y.B., Li, X.H., Li, Z.X., Wu, F.Y., 2007. Contrasting zircon Hf and O isotopes in the two episodes of Neoproterozoic granitoids in South China: implications for growth and reworking of continental crust. Lithos 96, 127–150.

Zheng, Y.F., Wu, R.X., Wu, Y.B., Zhang, S.B., Yuan, H.L., Wu, F.Y., 2008a. Rift melting of juvenile arc-derived crust: geochemical evidence from Neoproterozoic volcanic and granitic rocks in the Jiangnan Orogen, South China. Precambrian Research 163, 351–383.

Zheng, Y.F., Gong, B., Zhao, Z.F.,Wu, Y.B., Chen, F.K., 2008b. Zircon U–Pb age and O isotope evidence for Neoproterozoic low-(18) O magmatism during supercontinental rifting in South China: implications for the snowball earth event. American Journal of Science 308, 484–516.

Zhou, M. F., Yan, D. P., Kennedy, A. K., Li, Y., Ding, J., 2002. SHRIMP U–Pb zircon geochronological and geochemical evidence for Neoproterozoic arc-magmatism along the western margin of the Yangtze Block, South China. Earth and Planetary Science Letters 196(1-2), 51-67.

Zhou, J.C., Wang, X.L., Qiu, J.S., Gao, J.F., 2004. Geochemistry of Meso- and Neoproterozoic mafic–ultramafic rocks from northern Guangxi, China: arc or plume magmatism? Geochemical Journal 38, 139–152.

Zhou, J.B., Li, X.H., Ge, W.C., Liu, Y., 2007. Geochronology mantle source and geo-logical implications of neoproterozoic ultramafic rocks from Yuanbaoshan areaof Northern Guangxi. Geological Science and Technology Information 26 (1),11–18.

Zhou, J.C., Wang, X.L., Qiu, J.S., 2009, Geochronology of Neoproterozoic mafic rocks and sandstones from northeastern Guizhou, South China: Coeval arc magmatism and sedimentation. Precambrian Research 170 (1–2), 27-42.

Zhou, J. C.; Wang, X. L.; and Qiu, J. S. 2014. Neoproterozoic tectono-magmatic evolution of the Jiangnan orogen. Beijing, Science Press, 282 p. (in Chinese with English abstract).

Zhou, X.M., Zhou, H.B., Yang, J.D., Wang, Y.X. 1989. Sm-Nd isochron age of the ophiolite suite in Shexian County, Anhui Province and its geological significance. Chinese Science Bulletin 35, 208-212 (In Chinese with English abstract).

Zhou, X.M., Zhu, Y.H., 1992. Magma mixing in the Jiang-Shao fault zone and the Precambrian geology of both side of the Jiang-Shao zone (in Chinese with English abstract). Science in China Series B 22, 298–303.

Zhou, G.Q., Zou, H.B. 1996. Precambrian high-pressure metamorphic rocks within the collision zone of the Yangtze and Cathaysia blocks, China: jadeite/glaucophane-type facies. International Geological Review 38, 87-93.

Table Captions

Supplementary Table 1. Zircon age distributions for arc type igneous suites in the Jiangnan Orogen.

Supplementary Table 2. Zircon Hf distributions for arc type igneous suites in the Jiangnan Orogen.

Supplementary Table 3. Zircon age distributions for S-type granites in the central and southwest domains of the Jiangnan Orogen.

Supplementary Table 4. Zircon Hf and O isotope distributions for S-type granites in the central and southwest domains of the Jiangnan Orogen.

Supplementary Table 5. Whole rock geochemical data for S-type granites in the central and southwest domains of the Jiangnan Orogen.

Supplementary Table 6. Whole rock geochemical data for volcanic and intrusive assemblages within the Sibao and equivalent groups of the Jiangnan Orogen.

Supplementary Table 7. Whole rock Sr and Nd isotopes for S-type granites and igneous assemblages within the Sibao and equivalent groups of the Jiangnan Orogen.

Supplementary Table 8. Zircon age distributions for the Shuangxiwu/ Shuangqiaoshan/ Sibao and equivalent groups in the Jiangnan Orogen.

Supplementary Table 9. Zircon Hf isotope distributions for the Shuangxiwu/ Shuangqiaoshan/ Sibao and equivalent groups in the Jiangnan Orogen.

Supplementary Table 10. Zircon age distributions for the Heshangzhen/ Dengshan /Danzhou and equivalent groups in the Jiangnan Orogen.

Supplementary Table 11. Zircon Hf distributions for the Heshangzhen/ Dengshan /Danzhou and equivalent groups in the Jiangnan Orogen.

Figure Captions

Fig. 1. Geological sketch map of the Jiangnan orogenic belt, South China Craton (1: Shaoxing - Jiangshan - Pingxiang - Shuangpai fault; 2: Zhenghe - Dapu fault; 3: Northeast Jiangxi fault; 4: Jiujiang - Shitai fault; 5: Xiangtan-Miluo fault; 6: Tanlu fault; 7: Longmenshan - Ailaoshan - Songma fault; SECCLMVZ: Southeast China costal late Mesozoic volcanic zone).

Fig. 2. Time space plot showing age range of principal rock units and tectono-thermal events within the Jiangnan orogenic belt.

Fig. 3. Regional cross-sections for the Jiangnan Orogen, locations of cross-sections can be found in Fig. 1. Abbreviations: Pt3shx – Shuangxiwu Group; Pt3hsz – Heshangzhen Group; Pt3z – Sinian System; Pt3shs – Shuangqiaoshan Group; Pt3ds – Dengshan Group; Pt3sx – Shangxi Group; Pt3lk – Likou Group; Pt3l – Lengjiaxi Group; Pt3b – Banxi Group; Pt3sb – Sibao Group; Pt3dz – Danzhou Group.

Fig. 4. Representative field photos from the Jiangnan orogenic belt, (A) unconformity

between the Shuangxiwu and Heshangzhen groups, northeast Jiangnan; (B) unconformity between the Shangxi and Likou groups; (C) unconformity between the Shuangqiaoshan and Dengshan groups; (D) unconformity between the Lengjiaxi and Banxi groups; (E) tight folds developed in the Lengjiaxi Group; (F) unconformity between the Sibao and Danzhou groups; (G) sheared quarts porphyroblasts indicating dip–slip motion in the Sibao Group; (H) folded structures within the Sibao Group; (I) eastward shearing structures of jasper blocks developed within ophiolitic mélange within the Sibao Group; (J) pillow basalt in the Sibao Group; (K) diorite enclave within the Jiuling granitic pluton in the central Jiangnan domain; (L) sheared Sanfang S-type granitic pluton in the southwest domain. See Fig. 3 for abbreviations.

Fig. 5. A comparison of Zircon age spectra and zircon Hf isotopes of convergent plate margin igneous suites from various domains of the Jiangnan Orogen. Sources of data, (a) zircon age data from the northeast Jiangnan domain (Huaiyu Terrane) (Ye et al. 2007; Li et al., 2008a; Chen et al. 2009, 2016; Yao et al. 2016a); (b) zircon age data from the central and southwestern domains of the Jiangnan Orogen (Zhou et al. 2009; Zhang et al. 2012c, 2013a, 2013b; Zhao and Zhou 2013; Wang et al. 2014b; Zhang and Wang 2016; Yao et al. 2014a, 2015; 2016b; Cui et al., 2017; Chen et al., 2017; Xia et al. 2017; Sun et al. 2017); (c) zircon εHf(t) versus crystallization age diagram for the northeast domain (Huaiyu Terrane) (Li et al., 2009; Yao et al., 2016b); (d) zircon εHf(t) versus crystallization age diagram for the central and southwest domains (Zhang et al., 2013a; Yao et al., 2014a, 2015, 2016a; Cui et al., 2017; Sun et al., 2017); (e) zircon Hf model age histogram for the northeast domain; (f) zircon Hf model age histogram for central and southwest domains (Zhang et al., 2013a; Yao et al., 2014a, 2015, 2016a; Cui et al., 2017; Sun et al., 2017); Data used in plots given in Supplementary Table 1 and 2.

Fig. 6. (a) and (b) zircon age spectra (data sources: Li et al., 2003a; Wang et al., 2006;

Wu et al., 2006; Xue et al., 2010; Zhao et al., 2013; Sun et al., 2017; Xin et al., 2017; Deng et al., 2018; Yao et al., 2014a; Zhao et al., 2013; Ma et al., 2016); (c) and (d) zircon εHf(t) versus crystallization ages; (e) and (f) Hf models ages; (data sources: Li et al., 2003a; Wang et al., 2006; Wu et al., 2006; Zhao et al., 2013; Sun et al., 2017; Deng et al., 2018; Yao et al., 2014a; Zhao et al., 2013; Ma et al., 2016; Xin et al., 2017) for S-type granite intrusions in the central and southwest domains of the Jiangnan orogenic belt, respectively. Data used in plots given in Supplementary Tables 3 and 4.

Fig. 7. Primitive mantle-normalized incompatible element distribution spidergrams for (a) S-granite in the central Jiangnan domain (b) S-granite in the southwest Jiangnan domain, (the normalization values are from Sun and McDonough, 1989; McDonough and Sun, 1995); (Y + Nb)-Rb plot for (c) S-granite in the central Jiangnan domain (d) S-type granite in the southwest Jiangnan domain (after Pearce et al., 1984); Sources of data, central Jiangnan domain, Li et al., 2003a; Xin et al., 2017; Sun et al., 2017; Deng et al., 2018; Southwest domain, Li et al., 2003a; Wang et al., 2006; Yao et al., 2014a; Wei et al., 2018. Data used in plots given in Supplementary Tables 5.

Fig. 8. Plots of εHf(t) versus $\delta^{18}O$ for the magmatic zircons with concordant ages in the S–type granites from the central and southwest domains of the Jiangnan orogenic belt. (Wang et al., 2013d; Zhao, et al. 2013). Data used in plots given in Supplementary Table 4.

Fig. 9. (a) and (b), Hf–Th–Ta diagram (after Wood, 1980); (c), Ta/Yb–Th/Yb diagram (after Pearce, 1982), for Neoproterozoic igneous rocks from the Jiangnan orogenic belt. Data used in plots given in Supplementary Table 6. Sources of data: Chen et al., 2014b, 2017; Zhou et al., 2009; Li et al., 2008a, 2009; Wang et al., 2004, 2008b,

2014a, 2015; Yao et al., 2016a, 2016b, 2014a, 2015, 2014b; Ye et al., 2007; Zhang et al., 2013a, 2012b, 2012c, 2013b, 2015b, 2018; Zhang and Wang, 2016; Zhao and Zhou, 2013; Sun et al., 2017; Cui et al., 2017.

Fig. 10. (a) whole rock initial $^{87}Sr/^{86}Sr$ (t) versus crystallization ages and (b) whole rock εNd(t) isotopes for various igneous rocks from the Jiangnan orogenic belt. Data used in plots given in Supplementary Table 7. Sources of data: Chen and Jahn, 1998; Shen et al., 1992; Li et al., 2003a, 2009; Wang et al., 2006; Wu et al., 2006; Zhang et al., 2012c, 2013b; Zhang and Wang, 2016; Chen et al., 2014, 2017; Wei et al., 2018; Deng et al., 2018.

Fig. 11. A comparison of age spectra from pre-Nanhua succession in various locations of the Jiangnan Orogen. Sources of data, (a) Shangxi Group in the east segment of the central domain (Yin et al. 2013; Cui et al. 2015; Xu et al., 2014a; Wang et al., 2013c, 2014b); (b) Shuangqiaoshan Group in the central domain (Wang et al., 2013c, 2014b; Li et al., 2016b); (c) Lengjiaxi group in the west segment of the central domain (Wang et al. 2014b, 2016a; Li et al. 2016b; Yao et al., 2018); (d) Fanjinshan Group in southwest Jiangnan Orogen (Zhou et al. 2009; Wang et al., 2010, 2014b; Ma et al., 2016); (f) Sibao Group in southwest Jiangnan Orogen (Wang et al., 2012a; Yang et al., 2015; Su et al., 2018a). Data used in plots given in Supplementary Table 8.

Fig. 12. Depositional setting of the Lengjiaxi, Sibao and equivalent groups as inferred by discrimination plot of cumulative proportions vs. CA–DA of analyzed detrital zircons (after Cawood et al. 2012). (CA–DA: zircon crystallization ages minus deposition ages, which is also the lag time between zircon ages of crystallization and deposition. Field A: red field, convergent setting; Field B: blue field, collisional setting; Field C: green field, extensional setting). See text for discussion.

Fig. 13. A comparison of zircon Hf isotopes from pre-Nanhua succession in various locations of the Jiangnan Orogen. Sources of data, (a) Shangxi Group in the central Jiangnan Orogen (Yin et al. 2013; Cui et al. 2015; Xu et al., 2014a; Wang et al., 2013c, 2014b); (b) Shuangqiaoshan Group in the central Jiangnan Orogen (Wang et al., 2013c, 2014b; Li et al., 2016b; Yao et al., 2018); (c) Lengjiaxi Group in the central Jiangnan Orogen (Wang et al. 2014b, 2016a; Yan et al., 2015; Yao et al., 2018); (d) Fanjinshan Group in the southwest Jiangnan Orogen (Zhou et al. 2009; Wang et al., 2010, 2014b; Ma et al., 2016); (e) Sibao Group in the southwest Jiangnan Orogen (Wang et al., 2012a; Yang et al., 2015; Su et al., 2018a). Data used in plots given in Supplementary Table 9.

Fig. 14. A comparison of age spectra from the Nanhua successions in various locations of the Jiangnan Orogen. Sources of data, (a) Heshangzhen Group in the northeast domain (Yao et al. 2013; Wang et al., 2013a; Xu et al., 2014a); (b) Likou Group in the northeast segment of the central domain (Yin et al. 2013; Cui et al. 2015); (c) Dengshan Group in the central domain (Zhao and Zhou 2013; Zhang and Wang 2016; Yao et al. 2016; Wang et al. 2014b); (d) Banxi Group in the west segment of the central domain (Yan et al., 2015; Wang et al., 2017); (e) Xiajiang Group in the southwest domain (Wang et al., 2010, 2012b; Ma et al., 2016); (f) Danzhou Group in the southwest domain (Wang et al., 2013a; Yang et al., 2015; Su et al., 2018a). Data used in plots given in Supplementary Table 10.

Fig. 15. A comparison of zircon Hf isotopes from the Nanhua successions in various locations of the Jiangnan Orogen. (a) Heshangzhen Group in the northeast Jiangnan Orogen (Yao et al. 2013; Wang et al., 2013a; Xu et al., 2014a); (b) Likou Group in the central Jiangnan Orogen (Yin et al. 2013; Cui et al. 2015); (c) Dengshan Group in the central Jiangnan Orogen (Zhao and Zhou 2013; Zhang and Wang 2016; Yao et al. 2016;

Wang et al. 2014b); (d) Banxi Group in the central Jiangnan Orogen (Yan et al., 2015); (e) Xiajiang Group in the southwest Jiangnan Orogen (Wang et al., 2010, 2012b; Ma et al., 2016); (f) Danzhou Group in the southwest Jiangnan Orogen (Wang et al., 2013a; Yang et al., 2015; Su et al., 2018a). Data used in plots given in Supplementary Table 11.

Fig. 16. Tectonic model for the Jiangnan Orogen. See text for discussion.

Fig. 17. Distribution of Neoproterozoic trench-arc-basin systems and orogenic belts in South China.

Fig. 18. Schematic paleogeographic reconstructions showing position of the Cathaysia and Yangtze blocks in inferred super-continental reconstructions at Rodinia assembly at ca. 820 Ma (adapted from Torsvik, 2003 and Cawood et al., 2018). Abbreviations: CA – Cathaysia.